IRIS AperTO

UNIVERSITÀ DEGLI STUDI DI TORINO

AperTO - Archivio Istituzionale Open Access dell'Università di Torino

Multiple catalytic activities of human 17β-hydroxysteroid dehydrogenase type 7 respond differently to inhibitors.

This is the author's manuscript

Original Citation:

Availability:

This version is available http://hdl.handle.net/2318/1723195 since 2020-01-15T15:51:22Z

Published version:

DOI:10.1016/j.biochi.2019.12.012

Terms of use:

Open Access

Anyone can freely access the full text of works made available as "Open Access". Works made available under a Creative Commons license can be used according to the terms and conditions of said license. Use of all other works requires consent of the right holder (author or publisher) if not exempted from copyright protection by the applicable law.

(Article begins on next page)

13 December 2025

Multiple catalytic activities of human 17β-hydroxysteroid dehydrogenase type 7 respond differently to inhibitors

Terenzio Ferrante[a], Salvatore Adinolfi[a], Giulia D'Arrigo[a], Donald Poirier[b], Martina Daga[a], Marco Lucio Lolli[a], Gianni Balliano[a], Francesca Spyrakis[a], Simonetta Oliaro-Bosso[a*]

[a] Department of Science and Drug Technology, University of Torino, Via P. Giuria 9, 10125 - Turin, Italy.

[b] Laboratory of Medicinal Chemistry, CHU de Québec – Research Centre and Université Laval, 2705, boulevard Laurier T-4-50 Québec, Canada G1V 4G2

*Corresponding Author

Department of Science and Drug Technology, University of Torino, Via P. Giuria 9, 10125, Turin, Italy.

e-mail: simona.oliaro@unito.it

Abstract

Cholesterol biosynthesis is a multistep process in mammals that includes the aerobic removal of three methyl groups from the intermediate lanosterol; one from position 14 and two from position 4. During the demethylations at position 4, a 3-ketosteroid reductase catalyses the conversion of both 4-methylzymosterone and zymosterone to 4-methylzymosterol and zymosterol, respectively, restoring the alcoholic function of lanosterol, which is also maintained in cholesterol. Unlike other eukaryotes, mammals also use the same enzyme as an estrone reductase that can transform estrone (E1) into estradiol. This enzyme, named 17β-hydroxysteroid dehydrogenase type 7 (HSD17B7), is therefore a multifunctional protein in mammals, and one that belongs to both the HSD17B family, which is involved in steroid-hormone metabolism, and to the family of post-squalene cholesterol biosynthesis enzymes.

CHILD, Congenital hemidysplasia with ichthyosiform erythroderma and limb defects; DHT, dihydrotestosterone; E1, estrone; E2, estradiol; Erg27p, yeast 3-ketosteroid reductase; *ERG27,* gene encoding yeast 3-ketosteroid reductase; 17β-HSDs, 17β-hydroxysteroid dehydrogenases; HSD17B1, 17β-hydroxysteroid dehydrogenase type 1; HSD17B7, 17β-hydroxysteroid dehydrogenase type 7; 4-MZs, 4-methylzymosterone; 4-MFs, 4-methylfecosterone; Zs, zymosterone NSDHL, NADH sterol dehydrogenase-like; OS, 2,3-oxidosqualene; OSC, oxidosqualene cyclase; P, progesterone; SC4MOL, sterol C-4 methyl oxidase-like; SRD, short-chain dehydrogenase/reductase

In the present study, a series of known inhibitors of human HSD17B7's E1-reductase activity have been assayed for potential inhibition against 3-ketosteroid reductase activity. Surprisingly, the assayed compounds lost their inhibition activity when assayed in HepG2 cells that were incubated with radiolabelled acetate and against the recombinant overexpressed human enzyme incubated with 4-methylzymosterone (both radiolabelled and not). Preliminary kinetic analyses suggest a mixed or non-competitive inhibition on the E1-reductase activity, which is in agreement with Molecular Dynamics simulations. These results raise questions about the mechanism(s) of action of these possible inhibitors, the enzyme dynamic regulation and the interplay between the two activities.

Keywords

17β-Hydroxysteroid dehydrogenases

HSD17B7

Inhibitors

Molecular Dynamics

4-Methylzymosterone

Steroids

1. Introduction

Hydroxysteroid dehydrogenases (HSDs) are enzymes that belong to the short-chain dehydrogenase/reductase (SDR) superfamily and that catalyse the NAD(P)(H)-dependent oxidoreduction of hydroxy/keto groups. SDRs play a crucial role in the biosynthesis and inactivation of steroid hormones and in the metabolism of some non-steroidal compounds [1]. Fourteen mammalian 17β-HSDs have been identified so far, all belonging to the SDR superfamily, with the exception of 17β-HSD5, which is a member of the AKR

CHILD, Congenital hemidysplasia with ichthyosiform erythroderma and limb defects; DHT, dihydrotestosterone; E1, estrone; E2, estradiol; Erg27p, yeast 3-ketosteroid reductase; *ERG27,* gene encoding yeast 3-ketosteroid reductase; 17β-HSDs, 17β-hydroxysteroid dehydrogenases; HSD17B1, 17β-hydroxysteroid dehydrogenase type 1; HSD17B7, 17β-hydroxysteroid dehydrogenase type 7; 4-MZs, 4-methylzymosterone; 4-MFs, 4-methylfecosterone; Zs, zymosterone NSDHL, NADH sterol dehydrogenase-like; OS, 2,3-oxidosqualene; OSC, oxidosqualene cyclase; P, progesterone; SC4MOL, sterol C-4 methyl oxidase-like; SRD, short-chain dehydrogenase/reductase

(aldo-keto reductase) superfamily. Out of fourteen, the thirteen human 17β-HSDs differ in tissue distribution, subcellular localisation, cofactor and substrate specificities [2]. Only seven human 17β-HSDs (17β-HSD1, 17β-HSD4, 17β-HSD5, 17β-HSD8, 17β-HSD10, 17β-HSD11 and 17β-HSD14) have been structurally characterised. Isoforms 1, 4 and 11 are reported as dimers, 8, 10 and 14 as tetramers, while 5 (AKR1C3) as a monomer.

While the overall sequence identity between the various human SDR enzymes is generally about 15 - 30%, a comparison of the available crystallographic structures highlights a common Rossmann fold, which consists of seven-stranded parallel β-sheets surrounded by six parallel α-helices [3]. Conserved sequence motifs in human 17β-HSDs include the N-A-G and the glycine-rich T-G-xxx-G-x-G motifs, the cofactor binding site, which is important for the maintenance of the β-core, and the S-Y-K (Serine, Tyrosine, Lysine) catalytic triad [3]. The main structural differences that arise from a 3D-structure comparison mainly relate to the F-C segment and the variable C-terminal section. The N-terminal region also experiences significant differences in the sequence but maintains in all isoforms the typical Rossmann fold.

The 17β-HSD type 7 (HSD17B7) was first detected as a prolactin receptor-associated protein in rats [4]. The murine homologue has been described as a 17β-HSD due to its ability to catalyse the conversion of estrone (E1) to estradiol (E2). The detection of high expression levels in ovaries led to the assumption that HSD17B7 plays an important role in pregnancy [5].

The human enzyme is expressed in typical steroidogenic tissues, such as ovaries and testis, but also in the breast, prostate, liver and fetal brain [6,7,8]. It converts the less active E1 into the potent E2 and inactivates both the active dihydrotestosterone (DHT) and progesterone (P) into the weak 5α-androstane-3β, 17β-diol and 4-pregnen-3β-ol-20-one, respectively [9]. Marijanovic and other authors have demonstrated that this enzyme also participates in the post-squalene section of cholesterol biosynthesis, as a 3-ketosteroid reductase [7,10]. In this pathway, HSD17B7, together with the C-4 methyl oxidase (SC4MOL) and C-4 decarboxylase/C-3 dehydrogenase (NSDHL) enzymes, belongs to the C-4 demethylation apparatus, which catalyses the sequential removal of two-methyl groups at the sterol C-4 position. HSD17B7 plays the role of

CHILD, Congenital hemidysplasia with ichthyosiform erythroderma and limb defects; DHT, dihydrotestosterone; E1, estrone; E2, estradiol; Erg27p, yeast 3-ketosteroid reductase; *ERG27,* gene encoding yeast 3-ketosteroid reductase; 17β-HSDs, 17β-hydroxysteroid dehydrogenases; HSD17B1, 17β-hydroxysteroid dehydrogenase type 1; HSD17B7, 17β-hydroxysteroid dehydrogenase type 7; 4-MZs, 4-methylzymosterone; 4-MFs, 4-methylfecosterone; Zs, zymosterone NSDHL, NADH sterol dehydrogenase-like; OS, 2,3-oxidosqualene; OSC, oxidosqualene cyclase; P, progesterone; SC4MOL, sterol C-4 methyl oxidase-like; SRD, short-chain dehydrogenase/reductase

zymosterone reductase, catalysing the reduction of 4-methylzymosterone (4-MZs) in 4-methylzymosterol and of zymosterone (Zs) in zymosterol (Fig. 1). The former catalytic activity has been only indirectly proven up to now, but has not been shown in vitro yet [11].

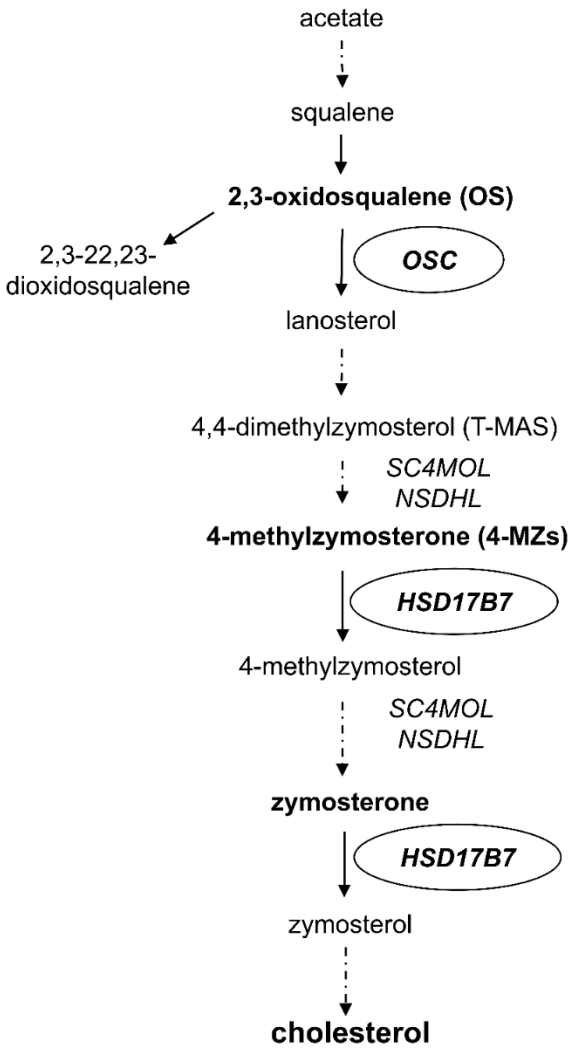

Fig. 1. Human-cholesterol biosynthetic pathway. OSC, oxidosqualene cyclase; T-MAS, 4,4-dimethyl zymosterol; SC4MOL, sterol C-4 methyl oxidase-like; NSDHL, NADH sterol dehydrogenase-like; HSD17B7, 17β-hydroxysteroid dehydrogenase type 7.

CHILD, Congenital hemidysplasia with ichthyosiform erythroderma and limb defects; DHT, dihydrotestosterone; E1, estrone; E2, estradiol; Erg27p, yeast 3-ketosteroid reductase; *ERG27,* gene encoding yeast 3-ketosteroid reductase; 17β-HSDs, 17β-hydroxysteroid dehydrogenases; HSD17B1, 17β-hydroxysteroid dehydrogenase type 1; HSD17B7, 17β-hydroxysteroid dehydrogenase type 7; 4-MZs, 4-methylzymosterone; 4-MFs, 4-methylfecosterone; Zs, zymosterone NSDHL, NADH sterol dehydrogenase-like; OS, 2,3-oxidosqualene; OSC, oxidosqualene cyclase; P, progesterone; SC4MOL, sterol C-4 methyl oxidase-like; SRD, short-chain dehydrogenase/reductase

A summary of the substrates of HSD17B7 that are involved in the metabolism of steroid hormones and in the biosynthesis of cholesterol is shown in Fig. 2.

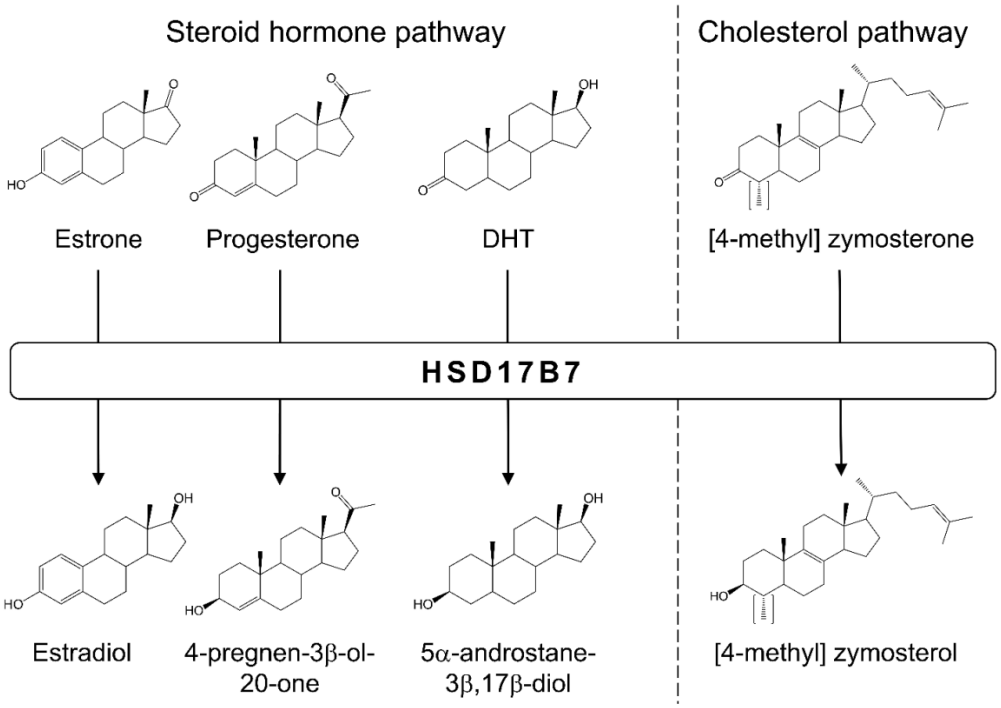

Fig. 2. Principal reductive reactions performed by human HSD17B7 in the steroid-hormone and cholesterol pathways.

Several cholesterol disorders are known to depend on the malfunctioning of a number of enzymes in post-squalene cholesterol biosynthesis in humans [12]. Two of these, SC4MOL deficiency and CHILD syndrome (related to mutations of the NSDHL gene), are associated to the enzymes that precede HSD17B7 in the three-step removal of the steroid-nucleus C-4 methyl group [12,13,14] (Fig. 1). For this reason, human HSD17B7 has been recognised as a novel candidate for inborn errors in cholesterol biosynthesis [10]. While no HSD17B7 deficiency has yet been identified, attempts at outlining the features of such a putative cholesterol disorder have been pursued via the development of animal models. Three independent studies on embryos

CHILD, Congenital hemidysplasia with ichthyosiform erythroderma and limb defects; DHT, dihydrotestosterone; E1, estrone; E2, estradiol; Erg27p, yeast 3-ketosteroid reductase; *ERG27,* gene encoding yeast 3-ketosteroid reductase; 17β-HSDs, 17β-hydroxysteroid dehydrogenases; HSD17B1, 17β-hydroxysteroid dehydrogenase type 1; HSD17B7, 17β-hydroxysteroid dehydrogenase type 7; 4-MZs, 4-methylzymosterone; 4-MFs, 4-methylfecosterone; Zs, zymosterone NSDHL, NADH sterol dehydrogenase-like; OS, 2,3-oxidosqualene; OSC, oxidosqualene cyclase; P, progesterone; SC4MOL, sterol C-4 methyl oxidase-like; SRD, short-chain dehydrogenase/reductase

from HSD17B7-deficient mice have reinforced the hypothesis that human HSD17B7 deficiency does indeed exist [11,15,16]. The embryonic lethality shown in these studies could explain why no case of human HSD17B7 deficiency has been reported up to now. In a mouse model with a recessive mutation of the *HSD17B7* gene, Stottmann *et al.* [11] observed the presence of embryo malformations (similar to those described in animal models of known human cholesterol disorder), the accumulation of 4-MZs (the enzyme substrate) in embryo brains and a dramatic reduction in Hedgehog signalling. The authors suggested that the altered embryo phenotype may depend on the toxic effect of 4-MZs accumulation toward the Hedgehog cascade, which is a critical process in correct embryo development. No inhibitor of HSD17B7-zymosterone-reductase activity is currently known, with the exception of fenhexamide, which has been reported to specifically inhibit the enzyme from *Botrytis cinerea* [17,18]. On the other hand, several effective E1-reductase inhibitors have been developed and reported in the literature [1,19,20].

In order to better characterise human HSD17B7, a series of HDS17B7 inhibitors, known for their ability to inhibit the conversion of E1 into E2, (Fig. 3) have been tested, in this work, for their potential to inhibit zymosterone-reductase activity in experiments with hepatoma HepG2 cells and recombinantly overexpressed human HSD17B7. The results suggest that the inhibitors could bind to a different pocket with respect to the orthosteric one and affect intrinsic enzyme dynamics. This hypothesis is further supported by the construction of the HSD17B7 model on the HSD17B1 crystallographic structure and by Molecular Dynamics and molecular docking simulations.

CHILD, Congenital hemidysplasia with ichthyosiform erythroderma and limb defects; DHT, dihydrotestosterone; E1, estrone; E2, estradiol; Erg27p, yeast 3-ketosteroid reductase; *ERG27,* gene encoding yeast 3-ketosteroid reductase; 17β-HSDs, 17β-hydroxysteroid dehydrogenases; HSD17B1, 17β-hydroxysteroid dehydrogenase type 1; HSD17B7, 17β-hydroxysteroid dehydrogenase type 7; 4-MZs, 4-methylzymosterone; 4-MFs, 4-methylfecosterone; Zs, zymosterone NSDHL, NADH sterol dehydrogenase-like; OS, 2,3-oxidosqualene; OSC, oxidosqualene cyclase; P, progesterone; SC4MOL, sterol C-4 methyl oxidase-like; SRD, short-chain dehydrogenase/reductase

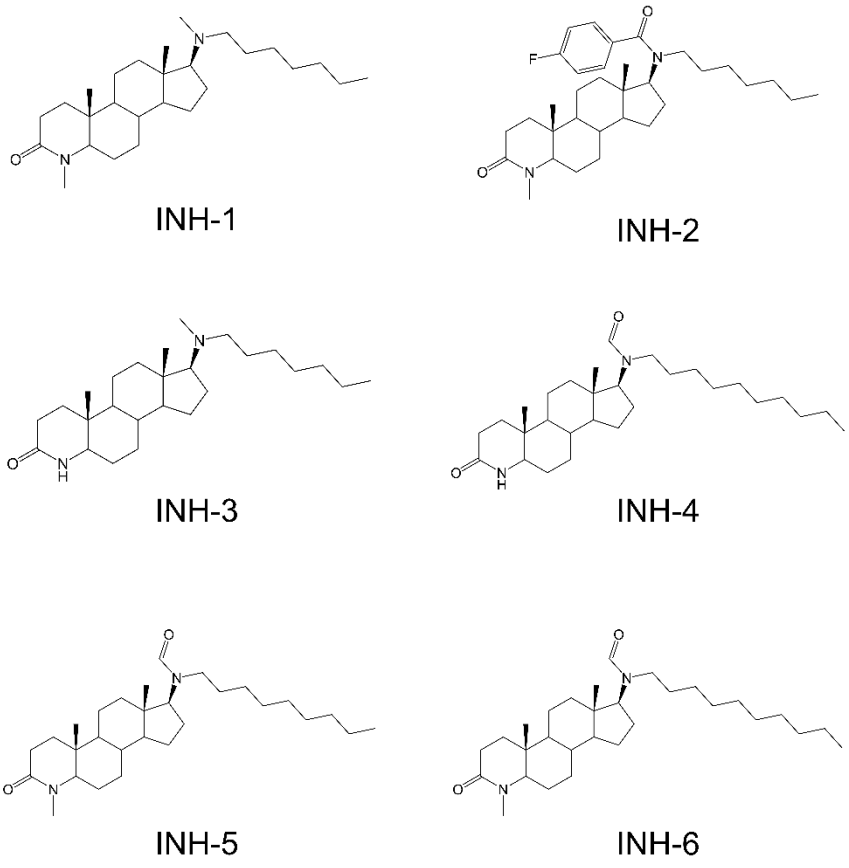

Fig. 3. Chemical structures of the HSD17B7 inhibitors used in this study. The compounds were described by Bellavance et al. [19] as 76 (INH-1), 34 (INH-2), 81 (INH-3), 80 (INH-4), 10 (INH-5), 11 (INH-6).

2. Material and methods

2.1 Chemicals

All the components for the buffers, culture media, cell culture supplements and bovine serum albumin (BSA) were obtained from Sigma-Aldrich (Italy), unless otherwise specified. All the solvents, ATP, $NADP^+$, glucose-6-phosphate, glucose-6-phosphate dehydrogenase, isopropyl β-D-1-thiogalactopyranoside (IPTG), E1, P and DHT were obtained from Alfa Aesar (Germany). The BCA protein assay kit was obtained from Fisher Scientific

CHILD, Congenital hemidysplasia with ichthyosiform erythroderma and limb defects; DHT, dihydrotestosterone; E1, estrone; E2, estradiol; Erg27p, yeast 3-ketosteroid reductase; *ERG27,* gene encoding yeast 3-ketosteroid reductase; 17β-HSDs, 17β-hydroxysteroid dehydrogenases; HSD17B1, 17β-hydroxysteroid dehydrogenase type 1; HSD17B7, 17β-hydroxysteroid dehydrogenase type 7; 4-MZs, 4-methylzymosterone; 4-MFs, 4-methylfecosterone; Zs, zymosterone NSDHL, NADH sterol dehydrogenase-like; OS, 2,3-oxidosqualene; OSC, oxidosqualene cyclase; P, progesterone; SC4MOL, sterol C-4 methyl oxidase-like; SRD, short-chain dehydrogenase/reductase

Italia. [2,4,6,7-^{3}H(N)]Estrone (250 µCi/9.25MBq, 94.0 Ci/mmol) and [1,2-^{14}C]acetate (50 µCi, 1.85MBq, 52.0 mCi/mmol) were obtained from Perkin-Elmer Italia.

The substrates 4-MZs, 4-methylfecosterone (4-MFs) and zymosterone (Zs) were prepared as previously reported [21]. Briefly, whole yeast *ERG27*-mutant cells were saponified and all non-saponifiable lipids were extracted using petroleum ether. Extracts were separated on thin layer chromatography (TLC) silica plates (ADAMANT UV254, Macherey-Nagel). Sterones were scraped off the plates and recovered from the silica eluting with diethyl ether. The purification proceeded further carrying out separating 4-MZs, 4-MFs and Zs by $AgNO_3$-TLC. Structural identification and sample purity of each sample were checked by GC-MS and NMR. Radiolabelled [^{14}C]4-MZs was prepared as previously reported [21]. Briefly, whole yeast *ERG27*-mutant cells were incubated for 3h at 30°C with [^{14}C]acetate. The separation of the labelled products was performed as described above.

2,3-Oxidosqualene (OS) and [^{14}C]-(3S)-2,3-oxidosqualene were prepared as previously described [22].

The studied compounds INH-1 {17β-[(N-heptyl)methylamino]-4-methyl-4-aza-5α-androstan-3-on}, INH-2 {17β-[(N-heptyl)-4-fluoro-phenylamido]-4-methyl-4-aza-5α-androstan-3-one}, INH-3 {17β-[(N-heptyl)methylamino]-4-aza-5α–androstan-3-one}, INH-4 {17β-[(N-decyl)formamido]-4-aza-5α–androstan-3-one}, INH-5 {17β-[(N-nonyl)formamido]-4-methyl-4-aza-5α–androstan-3-one} and INH-6 {17β-[(N-decyl)formamido]-4-methyl-4-aza-5α-androstan-3-one} (Fig. 3) were synthetised as previously reported [19].

2.2 Cell-culture conditions

Human hepatoma HepG2 cells were obtained from ATCC (ATCC® HB-8065). HepG2 cells were routinely maintained as monolayers in Dulbecco-modified Eagle medium (DMEM), which was supplemented with 10%

CHILD, Congenital hemidysplasia with ichthyosiform erythroderma and limb defects; DHT, dihydrotestosterone; E1, estrone; E2, estradiol; Erg27p, yeast 3-ketosteroid reductase; *ERG27,* gene encoding yeast 3-ketosteroid reductase; 17β-HSDs, 17β-hydroxysteroid dehydrogenases; HSD17B1, 17β-hydroxysteroid dehydrogenase type 1; HSD17B7, 17β-hydroxysteroid dehydrogenase type 7; 4-MZs, 4-methylzymosterone; 4-MFs, 4-methylfecosterone; Zs, zymosterone NSDHL, NADH sterol dehydrogenase-like; OS, 2,3-oxidosqualene; OSC, oxidosqualene cyclase; P, progesterone; SC4MOL, sterol C-4 methyl oxidase-like; SRD, short-chain dehydrogenase/reductase

(v/v) fetal bovine serum, 2% (v/v) penicillin-streptomycin and 0.03% L-glutamine. Cells were grown at 37°C in a humidified atmosphere (air 95%/ CO_2 5%).

Escherichia coli BL21 (DE3) Codon Plus RP cells [*E. coli B F- ompT hsdS (rB–mB–) dcm+ Tetr gal λ(DE3) endA Hte (argU proL Camr)*] were obtained from Agilent Technologies (Agilent N. 230255). Bacteria were grown in LB media supplemented with chloramphenicol (50 µg/mL) at 37 °C with continuous shaking.

2.3 Incorporation of [^{14}C]acetate into the non-saponifiable lipids of human HepG2 cells

The assay was performed as previously described [23]. Briefly, HepG2 cells were seeded into 24-well plates in DMEM (950 µl), which contained 10% (v/v) lipid-depleted adult bovine serum, at a density of 100,000 cells/well. After 24 h incubation, the inhibitors dissolved in absolute ethanol (5 µM, final concentration) were added and cells incubated for a further 3 h. The final concentration of ethanol in the culture medium did not exceed 0.4% (v/v); the same amount of ethanol was added to control cultures. Nevertheless, 0.4% ethanol had no observable significant effect on cell growth during the experiments. [^{14}C]acetate (1 µCi/well, 19.2 µM) was then added. After 3h incubation, the medium was removed and cells were treated with 0.1 M NaOH (500 µl) for 30 min. Phosphate buffer saline (500 µl) was added to each cell lysate and the mixture was saponified in 1 mL of methanolic KOH (10% w/v) for 30 min at 80°C. Non-saponifiable lipids were extracted twice with 1.5 mL of petroleum ether and separated on TLC-plates (ALUGRAM Xtra SIL G/ UV254, Macherey-Nagel) using cyclohexane/ethyl acetate (85:15 v/v) as the developing solvent and authentic standards of cholesterol, lanosterol, 2,3-22,23-dioxidosqualene, 2,3-oxidosqualene and squalene. Radioactivity in separated bands was quantified by integration using a radio-TLC Scanner (System 200 Imaging Scanner, Hewlett-Packard, USA). The amounts of radioactive label found in cholesterol and its biosynthetic post-squalene intermediates were expressed as percent of total counts found in non-saponifiable lipids.

CHILD, Congenital hemidysplasia with ichthyosiform erythroderma and limb defects; DHT, dihydrotestosterone; E1, estrone; E2, estradiol; Erg27p, yeast 3-ketosteroid reductase; *ERG27,* gene encoding yeast 3-ketosteroid reductase; 17β-HSDs, 17β-hydroxysteroid dehydrogenases; HSD17B1, 17β-hydroxysteroid dehydrogenase type 1; HSD17B7, 17β-hydroxysteroid dehydrogenase type 7; 4-MZs, 4-methylzymosterone; 4-MFs, 4-methylfecosterone; Zs, zymosterone NSDHL, NADH sterol dehydrogenase-like; OS, 2,3-oxidosqualene; OSC, oxidosqualene cyclase; P, progesterone; SC4MOL, sterol C-4 methyl oxidase-like; SRD, short-chain dehydrogenase/reductase

2.4 Oxidosqualene-cyclase (OSC) and zymosterone-reductase inhibition assays on human HepG2 lysates

Total HepG2 lysate was prepared as follows. HepG2 cells were incubated in complete medium DMEM with 10% fetal bovine serum in 100-mm-diameter dishes, grown to 70% confluence and maintained in DMEM with 10% (v/v) lipid-depleted adult bovine serum [24] for 24 h. HepG2 cells were then harvested by centrifugation at 1000 x g for 5 min and suspended in 100 mM phosphate buffer, pH 7.2, which contained freshly added protease inhibitors (Sigma-Aldrich). Cells were lysed by passage through a 22G x ½ needle 20 times. Protein concentration in cell lysates was measured using a BCA protein assay kit.

OSC activity was assayed by incubating cell lysates (about 3 mg of proteins) with the labeled [^{14}C]OS (1000 cpm, 25 µM) in the presence of the inhibitors (0.5 and 5 µM). Substrate and inhibitors were added as solutions in CH_2Cl_2 to test tubes in the presence of Tween-80 (0.5 mg/mL of final volume) and polidocanol (0.5 mg/mL of final volume). The solvent was evaporated under nitrogen. Then, substrate and inhibitors were dissolved in 100 mM phosphate buffer, pH 7.4, containing 0.2 mM EDTA and, after vigorous stirring, cell lysate was added (final volume 100 µL). After 1 h of incubation at 45°C the enzymatic reaction was stopped by adding 1 ml of KOH in methanol (10% w/v) and lipids were saponified at 80°C for 30 min. The extraction and separation of the non-saponifiable lipids were performed as described above. The conversion of the substrates into the labelled products was quantified by a radio-TLC scanner (System 200 Imaging Scanner, Hewlett-Packard, USA). The percentage of transformation was calculated by integration and used for the calculation of the enzyme activity.

Zymosterone-reductase activity was performed, as indicated above, by incubating cell lysates with labelled [^{14}C]4-MZs (2000 cpm, 150 µM) in the presence of the inhibitors (5 and 25 µM) for 3h at 37°C. 1 mM ATP, 5

CHILD, Congenital hemidysplasia with ichthyosiform erythroderma and limb defects; DHT, dihydrotestosterone; E1, estrone; E2, estradiol; Erg27p, yeast 3-ketosteroid reductase; *ERG27,* gene encoding yeast 3-ketosteroid reductase; 17β-HSDs, 17β-hydroxysteroid dehydrogenases; HSD17B1, 17β-hydroxysteroid dehydrogenase type 1; HSD17B7, 17β-hydroxysteroid dehydrogenase type 7; 4-MZs, 4-methylzymosterone; 4-MFs, 4-methylfecosterone; Zs, zymosterone NSDHL, NADH sterol dehydrogenase-like; OS, 2,3-oxidosqualene; OSC, oxidosqualene cyclase; P, progesterone; SC4MOL, sterol C-4 methyl oxidase-like; SRD, short-chain dehydrogenase/reductase

mM $MgCl_2$ and an NADPH-generating system (1mM $NADP^+$, 3 mM glucose-6-phosphate and 3 units of G-6-P dehydrogenase) were also added in the reaction mixture.

2.5 Enzymatic assays on recombinant human HSD17B7 overexpressed in *E. coli* BL21 (DE3) Codon Plus RP cells

pGEX-2T modified plasmid coding for human HSD17B7[25] (kindly provided by Prof. J. Adamski of the Institute of Experimental Genetics, Genome Analysis Centre, Neuherberg, Germany) was transformed into *E. coli* BL21 (DE3) Codon Plus RP cells. For protein expression, bacteria cells were grown in 2xYT media (16 g/L Tryptone,

10 g/L Yeast Extract, 5.0 g/L NaCl, Sigma-Aldrich), supplemented with ampicillin (0.1 mg/mL) 37°C, under continuous shaking. At OD600 nm = 0.6, expression was induced by IPTG (0.5 mM) at 24°C. Bacteria cells were harvested 2 h after induction by centrifugation (5000 x g for 15 min) and stored at -20°C until use.

The cell pellet (obtained from 20 mL of culture) was resuspended in 100 mM phosphate buffer, pH 8, which contained 1 mM EDTA, 0.05 % BSA and 10 µl protease inhibitor cocktail (Sigma-Aldrich) (Final volume 900 µl). Protein concentration was measured using a BCA protein assay kit.

Zymosterone-reductase activity was assayed by incubating the bacterial suspension (about 15 µg of proteins) with 4-MZs, 4-MFs and Zs (35 µM), in the presence of the inhibitors (0.1 to 50 µM). Substrate and inhibitors were added as solutions in CH_2Cl_2 to test tubes in the presence of triton X100 (0.5 mg/mL) and tween 80 (0.5 mg/mL). The solvent was evaporated under nitrogen. Then, substrate and inhibitors were dissolved in 100 mM Tris buffer, pH 7.4, containing 5 mM $MgCl_2$ and, after vigorous stirring, a NADPH-generating system (indicated above), and the bacterial suspension was added (final volume 100 µL). After 1 h of incubation at 37°C, the enzymatic reaction was stopped by adding 1 ml of KOH in methanol (10% w/v) and the lipids were

CHILD, Congenital hemidysplasia with ichthyosiform erythroderma and limb defects; DHT, dihydrotestosterone; E1, estrone; E2, estradiol; Erg27p, yeast 3-ketosteroid reductase; *ERG27,* gene encoding yeast 3-ketosteroid reductase; 17β-HSDs, 17β-hydroxysteroid dehydrogenases; HSD17B1, 17β-hydroxysteroid dehydrogenase type 1; HSD17B7, 17β-hydroxysteroid dehydrogenase type 7; 4-MZs, 4-methylzymosterone; 4-MFs, 4-methylfecosterone; Zs, zymosterone NSDHL, NADH sterol dehydrogenase-like; OS, 2,3-oxidosqualene; OSC, oxidosqualene cyclase; P, progesterone; SC4MOL, sterol C-4 methyl oxidase-like; SRD, short-chain dehydrogenase/reductase

saponified at 80°C for 30 min. The extraction and separation of non-saponifiable lipids was performed as indicated above.

Steroid-hormone reductase activity was performed, as described above, by incubating a bacterial suspension (about 15 µg of proteins) with P, E1 or DHT (35 µM) in the presence of the inhibitors (0.1 to 10 µM). The enzymatic reaction was terminated at 80°C for 10 min, and the mixture was extracted twice with 1.5 ml of diethyl ether. The extracts were spotted on TLC-plates and developed in chloroform/ethyl acetate (4:1 v/v). For both activities, substrate and product spots were visualised by sulfuric acid stain. Images were acquired using the ChemiDoc™ (Bio-Rad) Imaging System and individual band densities were integrated by Image Label™ software (Bio-Rad).

IC_{50} (half maximal inhibitory concentration) values were calculated using non-linear regression analyses of the residual activity *vs* the log of inhibitor concentration, on statistical software from Genstat (NAG, Oxford, U.K.). The values listed in Tables 4 and 5 are the means of three separate experiments, each with duplicate incubations.

For enzyme kinetics, a bacterial suspension (about 15 µg of proteins) was incubated, as described above with [^{3}H]E1 (2500 cpm), triton X100 (0.5 mg/mL), tween 80 (0.5 mg/mL) and an NADPH-generating system (indicated above) in 0.1 M Tris buffer, pH 7.4, which contained 5 mM $MgCl_2$ (final volume 100 µl), either in the absence or in the presence of INH-5, at either 0.4 or 1.5 µM.

Final substrate (E1) concentrations of 10, 25 and 100 µM were used and incubation times chosen in such a way as to result in transformation percentages that did not exceed 10% (a limit imposed in order to safely restrict the results to a range in which a linear relationship between product formation and reaction time can be obtained). The percentage conversion of the labelled E1 to E2 was estimated via the integration of radioactivity scans using a System 200 Imaging Scanner. The reaction rates that were obtained at the various substrate concentrations were fitted, using a non-linear regression method, to the Michaelis-Menten equation.

CHILD, Congenital hemidysplasia with ichthyosiform erythroderma and limb defects; DHT, dihydrotestosterone; E1, estrone; E2, estradiol; Erg27p, yeast 3-ketosteroid reductase; *ERG27,* gene encoding yeast 3-ketosteroid reductase; 17β-HSDs, 17β-hydroxysteroid dehydrogenases; HSD17B1, 17β-hydroxysteroid dehydrogenase type 1; HSD17B7, 17β-hydroxysteroid dehydrogenase type 7; 4-MZs, 4-methylzymosterone; 4-MFs, 4-methylfecosterone; Zs, zymosterone NSDHL, NADH sterol dehydrogenase-like; OS, 2,3-oxidosqualene; OSC, oxidosqualene cyclase; P, progesterone; SC4MOL, sterol C-4 methyl oxidase-like; SRD, short-chain dehydrogenase/reductase

2.6 Homology Modelling of HSD17B7

Homology modelling of HSD17B7 was performed using the SWISS-MODEL service [26], an integrated web-based modelling environment. According to the sequence alignment, the crystal structure of HSD17B1 was identified as the closest match to HSD17B7 and used as a template for homology modelling. In particular, the ternary complex of HSD17B1 with equilin and $NADP^+$ (PDB, 1EQU) [27] was used as template, being one of the SDR enzyme with the highest homology with the target. The same structure, complete and not mutated, was already used as template for homology modelling simulations by other authors [7].

A three-dimensional model was generated on the basis of the sequence alignment between the target protein and the template structure. The stereochemical validation of the predicted model was carried out by building the Ramachandran plot of the protein-backbone structure using the RAMPAGE server (http://mordred.bioc.cam.ac.uk/~rapper/rampage.php).

2.7 Molecular Docking of the putative HSD17B7-inhibitor binding site

Rigid molecular docking simulations were performed using GOLD suite version 5.5 [28]. The region of interest for the docking studies was set to contain all residues within a distance of 10 Å from a reference atom (NZ, Lys 176). GOLD default parameters were used, and the compound was subjected to 10 genetic algorithm runs using the CHEMPLP fitness function.

2.8 Molecular Dynamics simulations of the HSD17B7 model

Molecular Dynamics (MD) of the HSD17B7 model, in both the free and liganded form, was performed using GROMACS package version 4.6.1 [29]. Protein topology was built using the Amber99SB-ILDN force field [30], and the protein was solvated with the TIP3P water model [31], in a 12 Å cubic box. Prior to MD simulation,

CHILD, Congenital hemidysplasia with ichthyosiform erythroderma and limb defects; DHT, dihydrotestosterone; E1, estrone; E2, estradiol; Erg27p, yeast 3-ketosteroid reductase; *ERG27,* gene encoding yeast 3-ketosteroid reductase; 17β-HSDs, 17β-hydroxysteroid dehydrogenases; HSD17B1, 17β-hydroxysteroid dehydrogenase type 1; HSD17B7, 17β-hydroxysteroid dehydrogenase type 7; 4-MZs, 4-methylzymosterone; 4-MFs, 4-methylfecosterone; Zs, zymosterone NSDHL, NADH sterol dehydrogenase-like; OS, 2,3-oxidosqualene; OSC, oxidosqualene cyclase; P, progesterone; SC4MOL, sterol C-4 methyl oxidase-like; SRD, short-chain dehydrogenase/reductase

the system was subjected to energy minimisation over 5000 maximum steps with the steepest-descent algorithm. The system was then equilibrated in four subsequent steps: 500 ps in the NVT ensemble at 100 K, 200 K, 300 K, and 1 ns in the NPT ensemble, in order to reach the pressure-equilibrium condition. The integration step was set to 2 fs. The production run was carried out in the NVT ensemble at 300 K without any restraint for 1 μs. The two trajectories were analysed using utilities in the GROMACS suite, which includes root-mean-square-deviation (RMSD), root-mean-square-fluctuation (RMSF) and essential-dynamics (ED) analyses.

ED analyses were performed to identify the global and correlated motions within the trajectories [32]. The graphical representation of the motion described by each eigenvector is provided by the porcupine plots, which were generated using the Pymol script modevector.py (Pymol version 2.1.1). In order to visualise the motion, a cone that represents the direction of movement was drawn for each residue.

3. Results

3.1 Effect of known E1-reductase inhibitors on cholesterol biosynthesis in HepG2 cells

A series of HDS17B7 inhibitors, known for their ability to inhibit the conversion of E1 into E2 (compounds INH-1, INH-2 and INH-3**,** Fig. 3) [19], were tested for their zymosterone-reductase inhibiting capacity. The effectiveness of these molecules has previously been demonstrated in a whole-cell system (HSD17B7-transfected HEK-293 cells), where they were proven to decrease E1-reductase activity [19]. In order to assay their effect on cholesterol biosynthesis, hepatoma HepG2 cells were grown in a lipid-depleted medium and incubated with radioactive acetate for 3h in the presence of inhibitors. As a control, HepG2 cells were also incubated with radioactive acetate for 3h in the absence of inhibitors. After incubation, non-saponifiable

CHILD, Congenital hemidysplasia with ichthyosiform erythroderma and limb defects; DHT, dihydrotestosterone; E1, estrone; E2, estradiol; Erg27p, yeast 3-ketosteroid reductase; *ERG27,* gene encoding yeast 3-ketosteroid reductase; 17β-HSDs, 17β-hydroxysteroid dehydrogenases; HSD17B1, 17β-hydroxysteroid dehydrogenase type 1; HSD17B7, 17β-hydroxysteroid dehydrogenase type 7; 4-MZs, 4-methylzymosterone; 4-MFs, 4-methylfecosterone; Zs, zymosterone NSDHL, NADH sterol dehydrogenase-like; OS, 2,3-oxidosqualene; OSC, oxidosqualene cyclase; P, progesterone; SC4MOL, sterol C-4 methyl oxidase-like; SRD, short-chain dehydrogenase/reductase

lipids were separated by TLC and the distribution of radioactivity among the components was detected using an imaging scanner (Table 1).

Table 1. Incorporation of [^{14}C]acetate into the non-saponifiable lipids of HepG2 cells, in the presence of INH-1, INH-2 and INH-3 at 5 µM.

	Distribution of radioactivity incorporated into non-saponifiable lipids (%)						
	Squalene	Oxido squalene	Dioxido squalene	4-Methyl zymo sterone (4-Mz)	Lanosterol	4-Mono methyl sterols[a]	Cholesterol
Controls	0.42	29.36	0.66	0.24	19.68	10.02	39.62
INH-1	0.45	63.48	16.67	0.41	9.73	2.76	6.48
INH-2	0.46	32.93	0.78	0.67	51.56	3.12	10.48
INH-3	0.57	18.93	1.83	0.2	60.55	3.67	14.11

[a] TLC bands with Rf values ranging from lanosterol to cholesterol. Mean of three separate experiments, each with duplicate incubations. Maximum deviations from the mean were lower than 10%.

As reported in Table 1, no accumulation of radioactive 4-MZs was observed in the presence of any of the inhibitors. However, the distribution of radioactivity in the treated and control cells was different. INH-1 led to the accumulation of oxidosqualene and dioxidosqualene, suggesting that it caused the inhibition of OSC, an upstream enzyme that is involved in cholesterol biosynthesis.

INH-2 and INH-3 displayed cholesterol/lanosterol ratios that were reversed in the treated cells. This suggests that a post-lanosterol enzyme from the cholesterol pathway had been affected, whereas HSD17B7 had not. More experiments were performed in order to confirm this unexpected result. HepG2 cells were homogenised and cell lysates were incubated, either in the presence or absence of the inhibitors, with in-

CHILD, Congenital hemidysplasia with ichthyosiform erythroderma and limb defects; DHT, dihydrotestosterone; E1, estrone; E2, estradiol; Erg27p, yeast 3-ketosteroid reductase; *ERG27,* gene encoding yeast 3-ketosteroid reductase; 17β-HSDs, 17β-hydroxysteroid dehydrogenases; HSD17B1, 17β-hydroxysteroid dehydrogenase type 1; HSD17B7, 17β-hydroxysteroid dehydrogenase type 7; 4-MZs, 4-methylzymosterone; 4-MFs, 4-methylfecosterone; Zs, zymosterone NSDHL, NADH sterol dehydrogenase-like; OS, 2,3-oxidosqualene; OSC, oxidosqualene cyclase; P, progesterone; SC4MOL, sterol C-4 methyl oxidase-like; SRD, short-chain dehydrogenase/reductase

house radiolabelled purified 4-MZs or OS, which are the substrates of the HSD17B7 and OSC enzymes, respectively. The 4-Mz was used for the first time as a substrate in an in vitro activity assay. Indeed, the substrate is hardly commercially available and we synthetised it by an original fermentative procedure with a yeast strain engineered by our group.[21]

Considering that INH-2 and INH-3 presented similar results in the previous assay, it was decided to test either INH-2 or INH-3 in comparison with INH-1. For the HSD17B7 inhibition assay, we used INH-1 and INH-2 at 5 and 25 µM (Table 2).

Table 2. Incubation of HepG2 lysate with [^{14}C]4-MZs in the presence of INH-1 and INH-2 at 5 µM and 25 µM.

	Enzymatic activity (% of 4-MZs reduced to 4-methylzymosterol)	Inhibition (%)
Controls	18.8	-
INH-1		
5 µM	18.7	0.3
25 µM	18.2	2.9
INH-2		
5 µM	17.8	5.4
25 µM	17.6	6.4

Mean of three separate experiments, each with duplicate incubations. The maximum deviations from the mean were lower than 10%.

Table 2 shows that the conversion of the substrate into the product in the lipid extracts from treated HepG2 cell lysates was found to be comparable to that of the control lysates. Only negligible inhibitory effects, from both INH-1 and INH-2, on the zymosterone-reductase activity of HSD17B7 were observed even when the assay was carried out at a higher concentration (25 µM), thus confirming the data observed in the acetate-incorporation assay whit whole HepG2 cells (Table 1). Results obtained with cell lysate have to be considered

CHILD, Congenital hemidysplasia with ichthyosiform erythroderma and limb defects; DHT, dihydrotestosterone; E1, estrone; E2, estradiol; Erg27p, yeast 3-ketosteroid reductase; *ERG27,* gene encoding yeast 3-ketosteroid reductase; 17β-HSDs, 17β-hydroxysteroid dehydrogenases; HSD17B1, 17β-hydroxysteroid dehydrogenase type 1; HSD17B7, 17β-hydroxysteroid dehydrogenase type 7; 4-MZs, 4-methylzymosterone; 4-MFs, 4-methylfecosterone; Zs, zymosterone NSDHL, NADH sterol dehydrogenase-like; OS, 2,3-oxidosqualene; OSC, oxidosqualene cyclase; P, progesterone; SC4MOL, sterol C-4 methyl oxidase-like; SRD, short-chain dehydrogenase/reductase

preliminary, as the absence of marked inhibition by HSD17B7 inhibitors might be ascribed to the presence of other enzymes (insensitive to inhibitors) able to reduce 4-MZs to a corresponding alcohol. In order to avoid background activities for steroid or cholesterol metabolism, the subsequent HSD17B7 inhibition assays were performed using a recombinant human HSD17B7 overexpressed in bacteria, since bacteria are lacking these metabolic pathways (see chapter 3.3).

For the OSC inhibition assay, INH-1 and INH-3 were tested on OSC by incubating cell lysate with radioactive OS (Table 3). INH-1 showed an inhibitory effect of 80% when used at 5 μM, the concentration that caused remarkable levels of OS accumulation in intact cells. The assay was also carried out at a concentration that was ten-times lower, 0.5 μM, and no inhibitory effect was observed. However, INH-3 was confirmed to be completely ineffective as an OSC inhibitor (Table 3). INH-1 deserves further investigation since the OSC enzyme has recently been recognised as a possible anticancer therapy target [33,34].

Table 3. Incubation of HepG2 lysate with [^{14}C]OS in the presence of INH-1 and INH-3 at 0.5 μM and 5 μM.

	Enzymatic activity (% of OS[a] transformed into lanosterol)	Inhibition (%)
Controls	40.0	-
INH-1		
0.5 μM	38.5	3.9
5 μM	8.4	79.1
INH-3		
0.5 μM	41.3	0
5 μM	37.7	5.7

[a] OS: oxidosqualene. Mean of three separate experiments, each with duplicate incubations. Maximum deviations from the mean were lower than 10%.

CHILD, Congenital hemidysplasia with ichthyosiform erythroderma and limb defects; DHT, dihydrotestosterone; E1, estrone; E2, estradiol; Erg27p, yeast 3-ketosteroid reductase; *ERG27,* gene encoding yeast 3-ketosteroid reductase; 17β-HSDs, 17β-hydroxysteroid dehydrogenases; HSD17B1, 17β-hydroxysteroid dehydrogenase type 1; HSD17B7, 17β-hydroxysteroid dehydrogenase type 7; 4-MZs, 4-methylzymosterone; 4-MFs, 4-methylfecosterone; Zs, zymosterone NSDHL, NADH sterol dehydrogenase-like; OS, 2,3-oxidosqualene; OSC, oxidosqualene cyclase; P, progesterone; SC4MOL, sterol C-4 methyl oxidase-like; SRD, short-chain dehydrogenase/reductase

3.2 Enzymatic activities of HSD17B7 overexpressed in *E. coli*

Recombinant human HSD17B7 was overexpressed in *E. coli* BL21 (DE3) Codon Plus cells, according to the procedure described by D. Schuster *et al.* [25]. After enzyme expression, bacteria were harvested and suspended in a reaction buffer for the assay. Enzymatic assays were also performed as described by D. Schuster *et al.* [25]. Briefly, the bacterial suspension was incubated with substrates E1 and 4-MZs. The conversion of substrate to product was analysed and measured using a TLC-densitometric method. A negative control was carried out using *E. coli* cells, which were transformed with the plasmid without the *HSD17B7* gene to test for background activity. No transformation of E1 and 4-MZs into E2 and 4-methylzymosterol, respectively, was observed, thus validating this cell model (data not shown).

The enzymatic assays were extended to six different substrates, three of which belong to steroid-hormone metabolism, while three are involved in post-squalene sterol biosynthesis, in order to strengthen the comparison between the two metabolic activities in which the enzyme is involved.

DHT and P were used in addition to E1 as substrates of the steroid-hormone pathway [9]. On the other hand, 4-methylfecosterone, a substrate for Erg27p (yeast homologue of the human HSD17B7), was used as a third substrate for zymosterone-reductase activity, in addition to 4-MZs and Zs [35,36]. These latter three substrates were produced and purified in our laboratory [21].

A number of experiments were carried out to identify the proper assay conditions under which to test both enzymatic activities contemporaneously.

The use of detergents to solubilise the inhibitors was necessary and yet troublesome due to the significant differences in the response of the two enzyme activities in the presence of compounds such as tween 80 and triton X-100. A dose-dependent decrease of E1-reductase activity, from 0.01 to 0.1%, was observed upon treatment with triton X-100, whereas the same concentration range stimulated zymosterone-reductase

CHILD, Congenital hemidysplasia with ichthyosiform erythroderma and limb defects; DHT, dihydrotestosterone; E1, estrone; E2, estradiol; Erg27p, yeast 3-ketosteroid reductase; *ERG27,* gene encoding yeast 3-ketosteroid reductase; 17β-HSDs, 17β-hydroxysteroid dehydrogenases; HSD17B1, 17β-hydroxysteroid dehydrogenase type 1; HSD17B7, 17β-hydroxysteroid dehydrogenase type 7; 4-MZs, 4-methylzymosterone; 4-MFs, 4-methylfecosterone; Zs, zymosterone NSDHL, NADH sterol dehydrogenase-like; OS, 2,3-oxidosqualene; OSC, oxidosqualene cyclase; P, progesterone; SC4MOL, sterol C-4 methyl oxidase-like; SRD, short-chain dehydrogenase/reductase

activity in a dose-dependent manner (data not shown). After an exhaustive exploration of various conditions, the enzymatic assays were performed at 0.05% tween 80 and 0.05% triton X-100.

Another critical step in the procedure was the staining of the TLC plates used to separate the substrates and products of the enzymatic assays. A careful comparison of the different reagents was carried out and led to the selection of $FeCl_3$-sulfuric acid as the staining method as it elicits a similar chromatic response in all of the separate compounds. The results of the enzymatic assays with the six different substrates for the two HSD17B7 catalytic activities (3β-reductase and 17β-reductase activities) are shown in Table 4.

Table 4. Specific activity of human HSD17B7 expressed in bacteria with several substrates that belong to steroid-hormone metabolism and sterol/cholesterol biosynthesis.

HSD17B7 specific activity ± SE (nmol h^{-1} per mg protein)					
Steroid-hormone reduction			Sterol reduction		
Estrone (17β-reductase)	Progesterone (3β-reductase)	Dihydro testosterone (3β-reductase)	4-Methyl zymosterone (3β-reductase)	Zymosterone (3β-reductase)	4-Methylfecosterone (3β-reductase)
7.75 ± 0.74	8.74 ± 0.88	9.18 ± 0.91	12.66 ± 0.76	11.58 ± 0.93	13.18 ± 1.38

Mean of three separate experiments, each with duplicate incubations.

As shown in Table 4, the HSD17B7 activities were comparable for the three substrates belonging to the steroid-hormone metabolism and were able to transform both the natural substrates (4-MZs and Zs) and the yeast substrate 4-MFs equally efficiently.

CHILD, Congenital hemidysplasia with ichthyosiform erythroderma and limb defects; DHT, dihydrotestosterone; E1, estrone; E2, estradiol; Erg27p, yeast 3-ketosteroid reductase; *ERG27,* gene encoding yeast 3-ketosteroid reductase; 17β-HSDs, 17β-hydroxysteroid dehydrogenases; HSD17B1, 17β-hydroxysteroid dehydrogenase type 1; HSD17B7, 17β-hydroxysteroid dehydrogenase type 7; 4-MZs, 4-methylzymosterone; 4-MFs, 4-methylfecosterone; Zs, zymosterone NSDHL, NADH sterol dehydrogenase-like; OS, 2,3-oxidosqualene; OSC, oxidosqualene cyclase; P, progesterone; SC4MOL, sterol C-4 methyl oxidase-like; SRD, short-chain dehydrogenase/reductase

3.3 Comparative inhibitory assays on the multiple enzymatic activities of human HSD17B7 overexpressed in *E. coli*

The effect of five inhibitors (Fig. 3) was also tested, for each of the six substrates, on human HSD17B7 overexpressed in *E. coli*. As described above, INH-2 and INH-3 presented similar results with lysates and whole-cell assays (Tables 1 and 2), therefore INH-3 and INH-1 were selected for the following experiments.

In addition, three more molecules, the 17β-[(N-alkyl)formamido]-4-aza-androstanes (INH-4, INH-5 and INH-6, Fig. 3), which have previously been tested in intact HSD17B7-transfected HEK-293 cells and found to be active on E1-reductase activity [19], were analysed.

The results of the inhibition assays are shown in Table 5. Significant differences in the inhibitory effects of the various compounds on HSD17B7 enzymatic activities belonging to steroid-hormone metabolism or sterol/cholesterol metabolism were observed. Indeed, the steroid-hormone-reductase activity was highly sensitive to all of the five inhibitors, which demonstrated IC_{50} values that range from 0.41 to 6.02 μM. IC_{50} values confirmed the inhibition activity of the compounds shown previously [19]. On the other hand, no or little inhibitory effect was detected towards the sterol-reductase activity. Only compounds INH-1 and INH-4 weakly suppressed this activity, with inhibitions ranging from 25 to 45% at a concentration of 50 μM.

CHILD, Congenital hemidysplasia with ichthyosiform erythroderma and limb defects; DHT, dihydrotestosterone; E1, estrone; E2, estradiol; Erg27p, yeast 3-ketosteroid reductase; *ERG27,* gene encoding yeast 3-ketosteroid reductase; 17β-HSDs, 17β-hydroxysteroid dehydrogenases; HSD17B1, 17β-hydroxysteroid dehydrogenase type 1; HSD17B7, 17β-hydroxysteroid dehydrogenase type 7; 4-MZs, 4-methylzymosterone; 4-MFs, 4-methylfecosterone; Zs, zymosterone NSDHL, NADH sterol dehydrogenase-like; OS, 2,3-oxidosqualene; OSC, oxidosqualene cyclase; P, progesterone; SC4MOL, sterol C-4 methyl oxidase-like; SRD, short-chain dehydrogenase/reductase

Table 5. Inhibitory effect on the activity of human HSD17B7 expressed in bacteria with various substrates. The substrates were used at a 35 µM concentration. The inhibitors were tested at a concentration range from 0.1 to 10 µM for steroid-hormone-reductase activity and from 0.1 to 50 µM for sterol/cholesterol reductase activity.

	IC_{50} ± SE (µM)					
	Steroid-hormone reduction			Sterol reduction		
	Estrone (17β-reductase)	Progesterone (3β-reductase)	Dihydro testosterone (3β-reductase)	4-Methyl zymosterone (3β-reductase)	Zymosterone (3β-reductase)	4-Methyl fecosterone (3β-reductase)
INH-1	0.41 ± 0.04	0.60 ± 0.028	1.19 ± 0.05	>50 (30.58% ± 2.59)[a]	>50 (25.13% ± 6.47)[a]	>50 (41.97% ± 2.64)[a]
INH-3	0.96 ± 0.29	n.d.[b]	n.d.[b]	n.d.[b]	n.d.[b]	n.d.[b]
INH-4	1.12 ± 0.21	6.01 ± 0.29	5.78 ± 0.24	>50 (45.77% ± 13.49)[a]	>50 (25.08% ± 7.35)[a]	>50 (9.75% ± 9.78)[a]
INH-5	0.7 ± 0.13	3.16 ± 0.16	3.32 ± 0.55	>50 (17.0% ± 12.4)[a]	>50 (5.66% ± 2.25)[a]	>50 (9.41% ± 6.67)[a]
INH-6	2.91 ± 0.28	4.24 ± 0.16	3.96 ± 0.08	>50 (18.89% ± 4.63)[a]	>50 (15.32% ± 7.45)[a]	>50 (7.70% ± 1.86)[a]

[a] % of inhibition ± SE at 50 µM. [b]n.d.: not determined. Mean of three separate experiments, each with duplicate incubations.

CHILD, Congenital hemidysplasia with ichthyosiform erythroderma and limb defects; DHT, dihydrotestosterone; E1, estrone; E2, estradiol; Erg27p, yeast 3-ketosteroid reductase; *ERG27,* gene encoding yeast 3-ketosteroid reductase; 17β-HSDs, 17β-hydroxysteroid dehydrogenases; HSD17B1, 17β-hydroxysteroid dehydrogenase type 1; HSD17B7, 17β-hydroxysteroid dehydrogenase type 7; 4-MZs, 4-methylzymosterone; 4-MFs, 4-methylfecosterone; Zs, zymosterone NSDHL, NADH sterol dehydrogenase-like; OS, 2,3-oxidosqualene; OSC, oxidosqualene cyclase; P, progesterone; SC4MOL, sterol C-4 methyl oxidase-like; SRD, short-chain dehydrogenase/reductase

3.4 Enzyme kinetics

In order to unravel the reasons behind this difference in sensitivity, preliminary enzymatic kinetics analyses were carried out on the 17-ketosteroid reductase activity (transformation of E1 into E2) which is representative of the steroid-hormone reductase activity of the protein. INH-5 was selected for this assay as more active and selective with respect to the other two steroid-hormone substrates. Bacterial lysate was incubated with 10, 25 and 100 µM of E1 substrate in absence or presence of INH-5 (Fig. 3) at concentrations of 0.4 and 1.5 µM. These concentrations were selected because they are below and above the IC_{50} value. The double reciprocal plot of HSD17B7 enzymatic activity in the presence or absence of INH-5 is reported in Fig. 4. The intercepts with the axes suggested that INH-5 could behave as a mixed or a non-competitive inhibitor, implying that its binding site could be different to the orthosteric one. A more refined kinetics analysis will be carried out when the purified enzyme becomes available to confirm these findings.

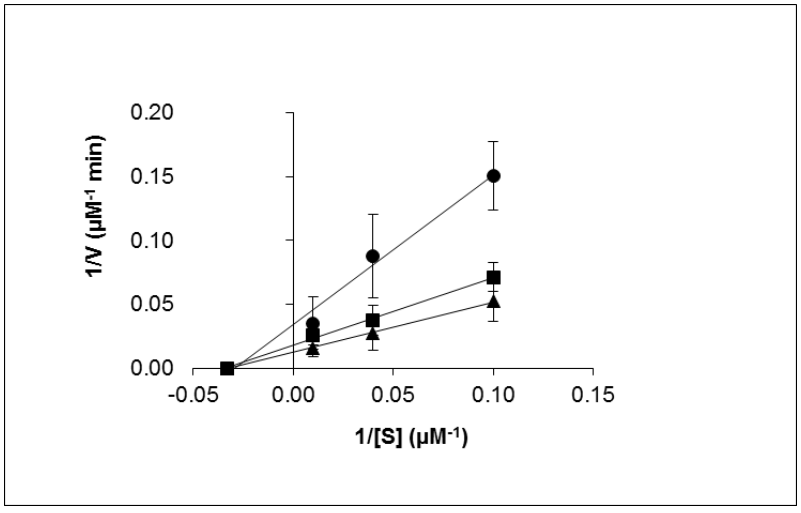

Fig. 4. Lineweaver–Burk analysis of the inhibition of human HSD17B7 by INH-5. E1-reductase activity was determined at different E1 concentrations (10, 25, and 100 µM), both in the absence (▲) and the presence of INH-5 at 0.4 µM (■) and 1.5 µM (●).

CHILD, Congenital hemidysplasia with ichthyosiform erythroderma and limb defects; DHT, dihydrotestosterone; E1, estrone; E2, estradiol; Erg27p, yeast 3-ketosteroid reductase; *ERG27,* gene encoding yeast 3-ketosteroid reductase; 17β-HSDs, 17β-hydroxysteroid dehydrogenases; HSD17B1, 17β-hydroxysteroid dehydrogenase type 1; HSD17B7, 17β-hydroxysteroid dehydrogenase type 7; 4-MZs, 4-methylzymosterone; 4-MFs, 4-methylfecosterone; Zs, zymosterone NSDHL, NADH sterol dehydrogenase-like; OS, 2,3-oxidosqualene; OSC, oxidosqualene cyclase; P, progesterone; SC4MOL, sterol C-4 methyl oxidase-like; SRD, short-chain dehydrogenase/reductase

3.5 Structure model of HSD17B7

The human 17β-HSDs of the SDR-family have very poor overall sequence identity (<25%), although some characteristic amino acid motifs are highly conserved [1]. Since there are no available crystal structures of HSD17B7, the dimeric type 1 was used for homology-based protein modelling; it is the best known and most commonly studied SDR member, it shares the biological function of HSD17B7 and has already been used as template for the same purpose [7]. The template structure is reported in Fig. 5. Three main structural features differentiate HSD17B1 from the other crystallographic SDR structures: a longer bFaG'-loop, an aG'-helix and a C-terminal helix [1]. In particular, the bFaG'-loop is defined as the *substrate-entry-loop* as it promotes and regulates the access of the cofactor and substrate to the active site [37].

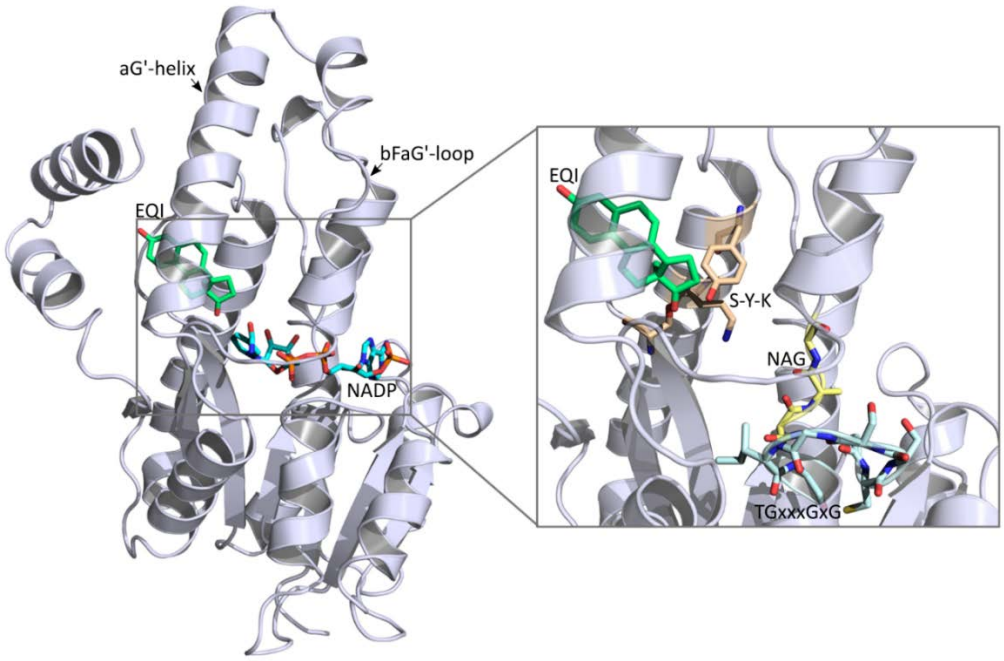

Fig. 5. HSD17B1 crystal structure. On the left: 3D structure of human HSD17B1 in complex with $NADP^+$, in cyan, and equilin (EQI), in green (PDB code: 1EQU). HSD17B1 is shown as cartoons and both EQI and $NADP^+$ as capped sticks. Loops and helices are labelled. On the right: a zoomed-in image of the region cofactor and

CHILD, Congenital hemidysplasia with ichthyosiform erythroderma and limb defects; DHT, dihydrotestosterone; E1, estrone; E2, estradiol; Erg27p, yeast 3-ketosteroid reductase; *ERG27,* gene encoding yeast 3-ketosteroid reductase; 17β-HSDs, 17β-hydroxysteroid dehydrogenases; HSD17B1, 17β-hydroxysteroid dehydrogenase type 1; HSD17B7, 17β-hydroxysteroid dehydrogenase type 7; 4-MZs, 4-methylzymosterone; 4-MFs, 4-methylfecosterone; Zs, zymosterone NSDHL, NADH sterol dehydrogenase-like; OS, 2,3-oxidosqualene; OSC, oxidosqualene cyclase; P, progesterone; SC4MOL, sterol C-4 methyl oxidase-like; SRD, short-chain dehydrogenase/reductase

substrate-binding region, where the conserved motifs T-G-xxx-G-x-G (pale cyan), N-A-G (pale yellow) and the S-Y-K catalytic triad (light orange) are located. Only one monomer has been reported for clarity.

The alignment of type 1 and type 7 resulted in 18% sequence identity. The crystal structure of the homo-dimeric HSD17B1 in binding with equilin and $NADP^+$ (PDB code:1EQU) [27], was chosen as the template for homology-based protein modelling, which was performed using the Swiss-Model server. The resulting 3D protein model has two highly disordered loops in each monomer (L1 and L3 in Fig. 6). Loop L1 is located above the active site and contains residues 90-130, which correspond to the longer, non-matching region of the primary sequence, while the loop L3 of the C-terminal region contains the residues 274-293 (Fig. 6 and Fig. S1). The quality of the predicted 3D model was assessed using the online tool RAMPAGE. The Ramachandran plot revealed that, of the 616 residues, 86.9% were in the favoured 9.0% in the allowed, and 4.0% in the disallowed region, proving that the model is quite acceptable (Fig. S2).

With respect to the original structure, the carboxy-terminal region of the protein appeared more disordered, and, reasonably, more flexible. However, the previously mentioned HSD17B1 structural peculiarities were quite conserved. The bFaG'-loop (L2 in the HSD17B7 model, Figure 6) was, in fact, still present, as well as the aG'-helix (H1, Figure 6), even if shorter, and the C-terminal helix (H2, Figure 6).

CHILD, Congenital hemidysplasia with ichthyosiform erythroderma and limb defects; DHT, dihydrotestosterone; E1, estrone; E2, estradiol; Erg27p, yeast 3-ketosteroid reductase; *ERG27,* gene encoding yeast 3-ketosteroid reductase; 17β-HSDs, 17β-hydroxysteroid dehydrogenases; HSD17B1, 17β-hydroxysteroid dehydrogenase type 1; HSD17B7, 17β-hydroxysteroid dehydrogenase type 7; 4-MZs, 4-methylzymosterone; 4-MFs, 4-methylfecosterone; Zs, zymosterone NSDHL, NADH sterol dehydrogenase-like; OS, 2,3-oxidosqualene; OSC, oxidosqualene cyclase; P, progesterone; SC4MOL, sterol C-4 methyl oxidase-like; SRD, short-chain dehydrogenase/reductase

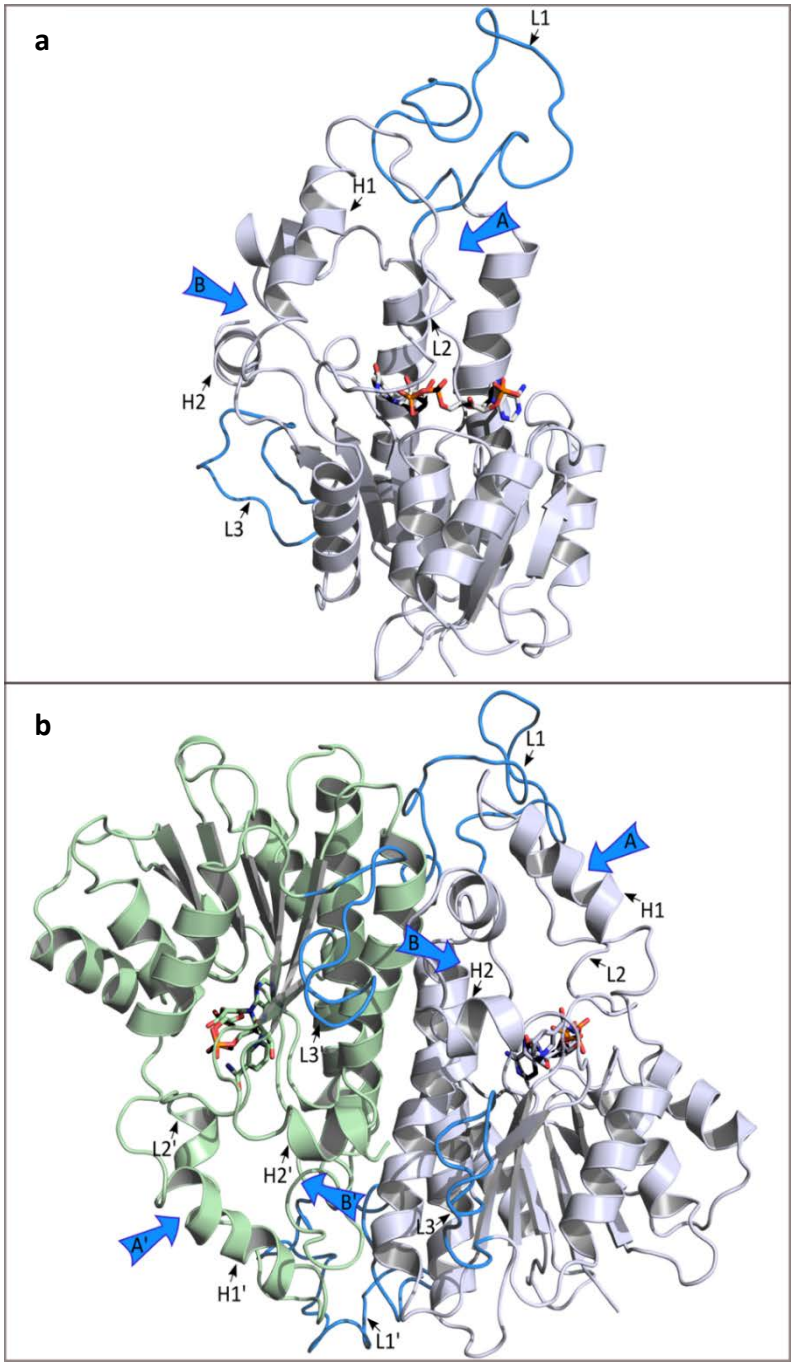

Fig. 6. Three-dimensional structure of the modelled HSD17B7 in the presence of cofactor $NADP^+$. a) Front side of the monomeric HSD17B7 model with the two possible accesses (A and B) pointed out by arrows. b) Rear side of the HSD17B7 model in dimeric form. Monomers A and B are coloured grey and green,

CHILD, Congenital hemidysplasia with ichthyosiform erythroderma and limb defects; DHT, dihydrotestosterone; E1, estrone; E2, estradiol; Erg27p, yeast 3-ketosteroid reductase; *ERG27,* gene encoding yeast 3-ketosteroid reductase; 17β-HSDs, 17β-hydroxysteroid dehydrogenases; HSD17B1, 17β-hydroxysteroid dehydrogenase type 1; HSD17B7, 17β-hydroxysteroid dehydrogenase type 7; 4-MZs, 4-methylzymosterone; 4-MFs, 4-methylfecosterone; Zs, zymosterone NSDHL, NADH sterol dehydrogenase-like; OS, 2,3-oxidosqualene; OSC, oxidosqualene cyclase; P, progesterone; SC4MOL, sterol C-4 methyl oxidase-like; SRD, short-chain dehydrogenase/reductase

respectively. Protein is shown as cartoons, the cofactor as capped sticks, and the most flexible loops are coloured blue. Key loops and helices are labelled.

3.6 Putative inhibitor binding site

No structural evidence on the binding mode of 4-MZs in the enzyme's orthosteric site is available. Its large dimensions led us to suggest that a different access route than the bFaG' substrate-entry-loop, which is presumable used by E1 and the cofactor (access A in Fig. 6), could be exploited to reach the active site. A possible access route (access B in Fig. 6) was identified towards the back, near the C-terminal helix of the HSD17B7 model. Assuming that both E1 and 4-MZs bind to the same catalytic site, and considering the non-competitive nature of the inhibitors, it was hypothesised that the inhibitors may be able to interfere with the enzyme's activity, and most likely affect the dynamics of the access route that is exploited by E1, while having less of an effect on the access of 4-MZ compounds. In order to achieve further insight into the possible binding site of the inhibitors, a pocket search with the FLAPsite algorithm was implemented in FLAP [38] (www.moldiscovery.com). Six pockets were identified in the model of the HSD17B7 dimer complexed with cofactor $NADP^+$ (Fig. 7). Pockets 1 and 1' correspond to the active site of each monomer. These pockets host the catalytic triad and, in the template, are occupied by the cognate equilin. It is probable that all of the steroid hormone-related molecules bind here. Docking simulation for E1, 4-MZ, DHT and P were performed in Pocket 1. In all the cases reliable poses were obtained, with the compounds exposing the keto group to the catalytic residues (data not shown). Pockets 2 and 2' are close to the active sites and to the C-terminal helices and could be exploited by 4-MZs to enter the active site. Pocket 3 is located at the dimer interface, is quite close to the active sites and surrounded by the two C-terminal helices. Pocket 4 is located on the opposite site in an exposed region of one monomer. A pocket corresponding to pocket 3 was already predicted to be a possible additional binding site for apigenin, known to inhibit the HSD17B1 enzyme [39].

CHILD, Congenital hemidysplasia with ichthyosiform erythroderma and limb defects; DHT, dihydrotestosterone; E1, estrone; E2, estradiol; Erg27p, yeast 3-ketosteroid reductase; *ERG27,* gene encoding yeast 3-ketosteroid reductase; 17β-HSDs, 17β-hydroxysteroid dehydrogenases; HSD17B1, 17β-hydroxysteroid dehydrogenase type 1; HSD17B7, 17β-hydroxysteroid dehydrogenase type 7; 4-MZs, 4-methylzymosterone; 4-MFs, 4-methylfecosterone; Zs, zymosterone NSDHL, NADH sterol dehydrogenase-like; OS, 2,3-oxidosqualene; OSC, oxidosqualene cyclase; P, progesterone; SC4MOL, sterol C-4 methyl oxidase-like; SRD, short-chain dehydrogenase/reductase

Moreover, being close to the active site of both monomers, this pocket could reasonably host non-competitive ligands that can influence HSD17B7 catalytic activity.

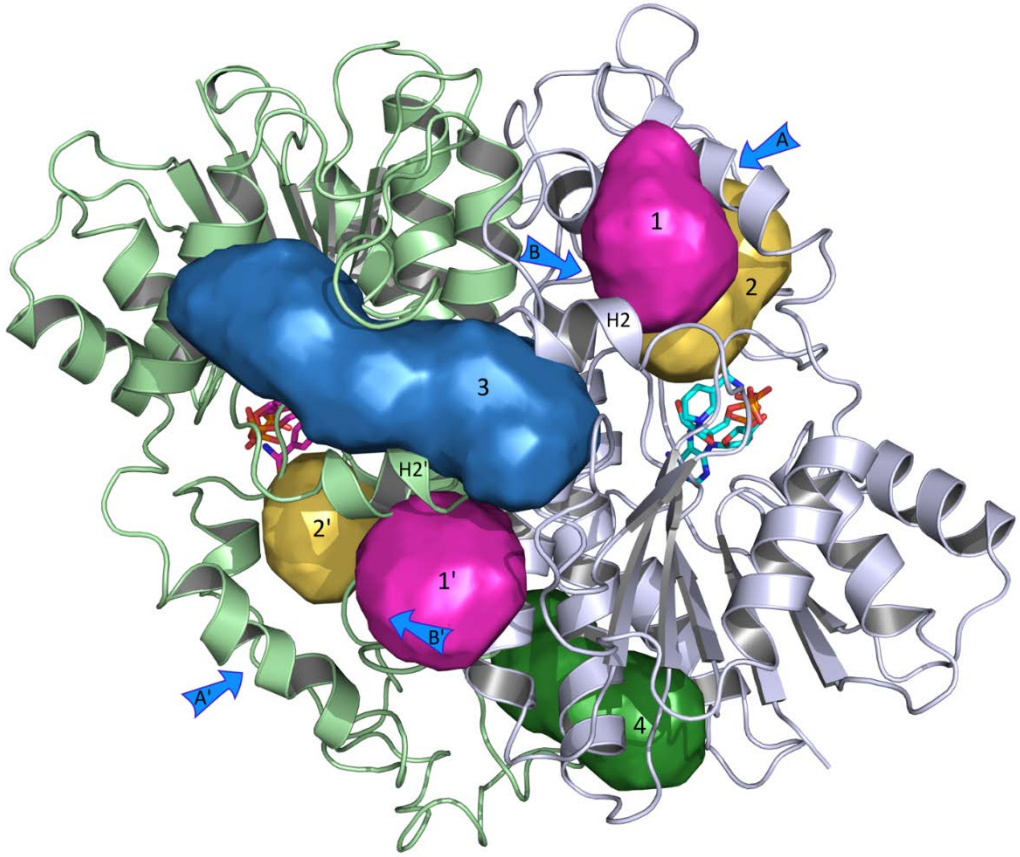

Fig. 7. Pockets detected in the HSD17B7 model by the FLAPsite algorithm [40]. The protein, in the homodimeric state, is shown as cartoons and the cofactor as capped sticks. Pockets, access routes and C-terminal helices are labelled.

INH-5 (named as "ligand" in the following), which was previously tested in the kinetic enzymatic assays, was chosen as the most representative compound and was docked in pocket 3 using the GOLD software. Having all the compounds the same scaffold, we hypothesized they should share the same binding mode. The ligand pose had a good docking score and a good interaction pattern with the surrounding residues. It was thus

CHILD, Congenital hemidysplasia with ichthyosiform erythroderma and limb defects; DHT, dihydrotestosterone; E1, estrone; E2, estradiol; Erg27p, yeast 3-ketosteroid reductase; *ERG27,* gene encoding yeast 3-ketosteroid reductase; 17β-HSDs, 17β-hydroxysteroid dehydrogenases; HSD17B1, 17β-hydroxysteroid dehydrogenase type 1; HSD17B7, 17β-hydroxysteroid dehydrogenase type 7; 4-MZs, 4-methylzymosterone; 4-MFs, 4-methylfecosterone; Zs, zymosterone NSDHL, NADH sterol dehydrogenase-like; OS, 2,3-oxidosqualene; OSC, oxidosqualene cyclase; P, progesterone; SC4MOL, sterol C-4 methyl oxidase-like; SRD, short-chain dehydrogenase/reductase

chosen for the following analyses (Fig. 8). The ligand appeared to be arranged in a folded shape that oriented the alkyl chain inward, while exposing the endocyclic amide to the solvent. H-bonds were formed with the side chain of Arg175 on monomer B and with the backbone of Lys176 on monomer A. Slight hydrophobic interactions were made with Ala288 on chain B, and with part of the side-chain of Lys176 on monomer A.

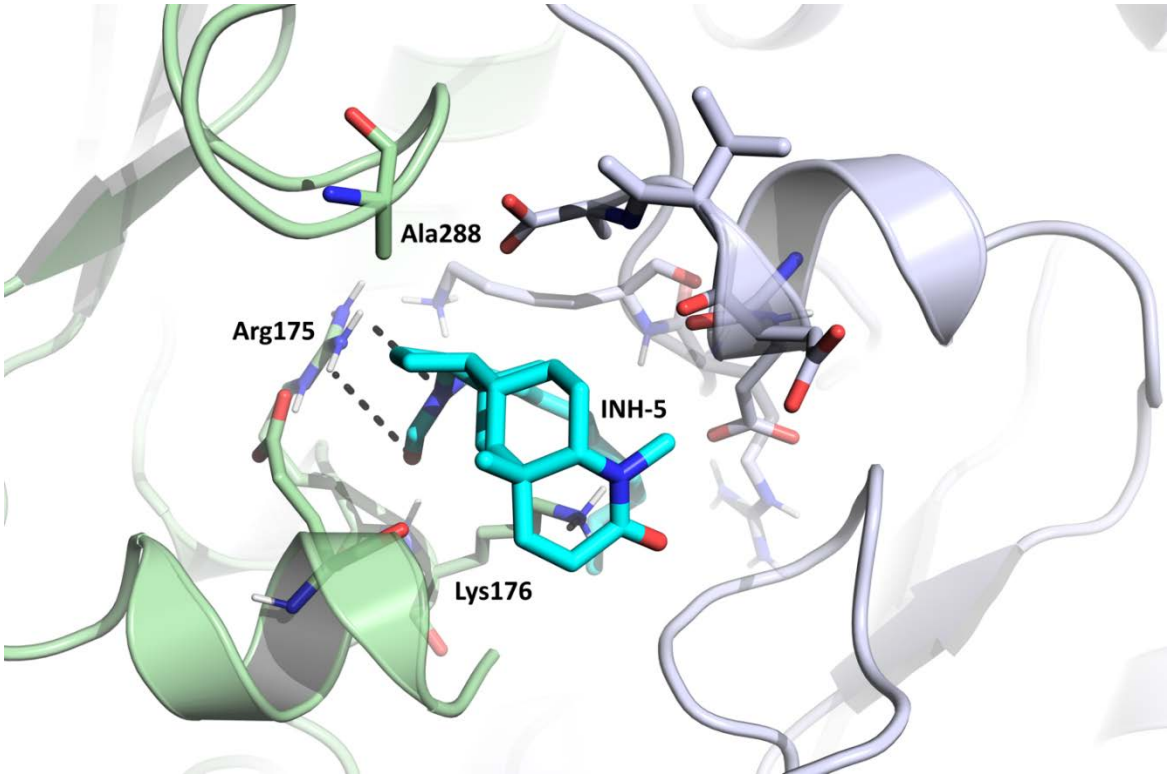

Fig. 8. Binding pose of compound INH-5 in pocket 3 at the dimer interface. Compound INH-5 and the residues lining the pocket are shown as capped sticks, H-bonds as dashed lines and the protein as cartoons. Residues that interact with the ligand are labelled.

3.7 Dynamics of HSD17B7 in the free and liganded state

In order to study the conformational stability of the HSD17B7 model (free state) and the complex with INH-5 (liganded state), a 1 μs-long Molecular Dynamics (MD) simulation was carried out for both states.

CHILD, Congenital hemidysplasia with ichthyosiform erythroderma and limb defects; DHT, dihydrotestosterone; E1, estrone; E2, estradiol; Erg27p, yeast 3-ketosteroid reductase; *ERG27,* gene encoding yeast 3-ketosteroid reductase; 17β-HSDs, 17β-hydroxysteroid dehydrogenases; HSD17B1, 17β-hydroxysteroid dehydrogenase type 1; HSD17B7, 17β-hydroxysteroid dehydrogenase type 7; 4-MZs, 4-methylzymosterone; 4-MFs, 4-methylfecosterone; Zs, zymosterone NSDHL, NADH sterol dehydrogenase-like; OS, 2,3-oxidosqualene; OSC, oxidosqualene cyclase; P, progesterone; SC4MOL, sterol C-4 methyl oxidase-like; SRD, short-chain dehydrogenase/reductase

The backbone root-mean-square deviation (RMSD) profile showed that the free form reaches equilibrium after about 200 ns and remained stable for rest of the simulation (Fig. S3a pink line). On the other hand, the RMSD increased over time in the liganded state (Fig. S3b light-purple line). This significant instability could be attributed to the enhanced flexibility of the loop elements in the presence of the ligand. Indeed, the removal of the most flexible loops (L1 and L3 on the first monomer and L1' and L3' on the second monomer) led to a more stable RMSD profile (magenta and purple lines in Fig. S3a and S3b, respectively).

The root-mean-square fluctuation (RMSF) of the two states was also determined (Fig. S4). As expected, the highest mobility was associated with the L1/L1' and L3/L3' loops and with the C-terminal H2/H2' alpha-helices surrounding the ligand. An essential dynamic analysis was performed [41], to further investigate how the ligand affected the stability of the protein and to distinguish the essential motions that characterised the two forms. The first 300 nanoseconds were discarded from both trajectories and the most flexible loops were removed from the analysis in order to ensure that the system was well-equilibrated. The contribution to the variance provided by the first ten eigenvectors is reported in Table S1. Overall, they described 72% of the total variance in the liganded state, and 69% in the free state. Furthermore, the first eigenvector contributed 28% of the total fluctuations in the liganded state, and 24% in the free state and, in both cases, the first three eigenvectors accounted for almost 50% of the total variance. The projections of the two trajectories on the plane, defined by the two first eigenvectors of the covariance matrix, showed that the free form appears to be confined to a narrower region than the liganded form (Fig. S5). This most likely indicated that the extension degree of essential motions in the free state is lower than that in the liganded state. This is also shown in Fig. 9, which reports the structural deformations given by the first eigenvector.

CHILD, Congenital hemidysplasia with ichthyosiform erythroderma and limb defects; DHT, dihydrotestosterone; E1, estrone; E2, estradiol; Erg27p, yeast 3-ketosteroid reductase; *ERG27,* gene encoding yeast 3-ketosteroid reductase; 17β-HSDs, 17β-hydroxysteroid dehydrogenases; HSD17B1, 17β-hydroxysteroid dehydrogenase type 1; HSD17B7, 17β-hydroxysteroid dehydrogenase type 7; 4-MZs, 4-methylzymosterone; 4-MFs, 4-methylfecosterone; Zs, zymosterone NSDHL, NADH sterol dehydrogenase-like; OS, 2,3-oxidosqualene; OSC, oxidosqualene cyclase; P, progesterone; SC4MOL, sterol C-4 methyl oxidase-like; SRD, short-chain dehydrogenase/reductase

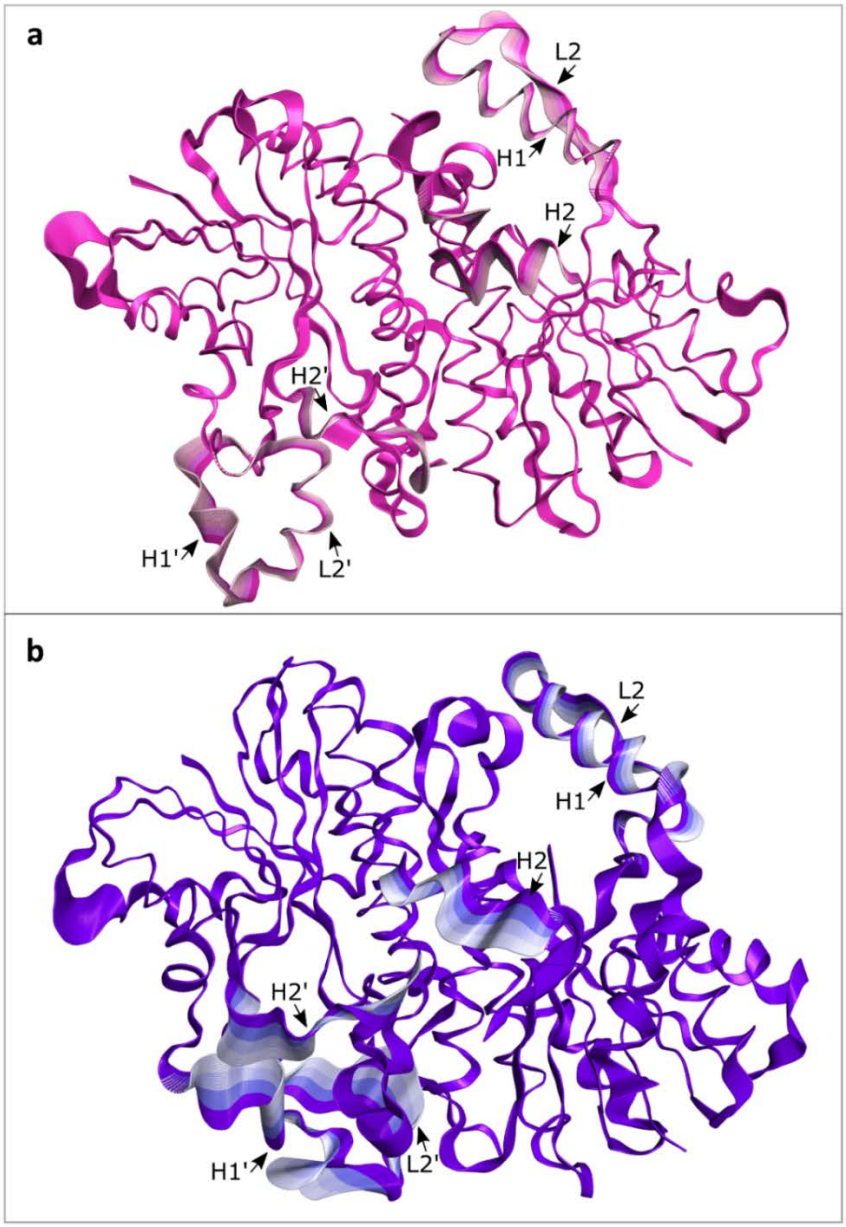

Fig. 9. Principal motions along the first eigenvector. The motions described by the first eigenvector are shown for the free (**a**) and the liganded (**b**) form, complexed with INH-5 (the ligand has been removed for clarity). The direction of motion is represented by a scale of colours, from darkest to lightest, while the magnitude of motion correlates to the amplitude of the cartoon. The structural elements involved in the greater motions are labelled.

CHILD, Congenital hemidysplasia with ichthyosiform erythroderma and limb defects; DHT, dihydrotestosterone; E1, estrone; E2, estradiol; Erg27p, yeast 3-ketosteroid reductase; *ERG27,* gene encoding yeast 3-ketosteroid reductase; 17β-HSDs, 17β-hydroxysteroid dehydrogenases; HSD17B1, 17β-hydroxysteroid dehydrogenase type 1; HSD17B7, 17β-hydroxysteroid dehydrogenase type 7; 4-MZs, 4-methylzymosterone; 4-MFs, 4-methylfecosterone; Zs, zymosterone NSDHL, NADH sterol dehydrogenase-like; OS, 2,3-oxidosqualene; OSC, oxidosqualene cyclase; P, progesterone; SC4MOL, sterol C-4 methyl oxidase-like; SRD, short-chain dehydrogenase/reductase

The picture clearly shows that the presence of the ligand strongly affected protein stability, particularly for the structural elements surrounding the active-site regions of both chain A and B; H1 and L2, and H1' and L2', respectively. Interestingly, while the C-terminal helix of both chains A and B underwent a significant rearrangement in the liganded state, only small adjustments were identified in the free form. This may suggest that the ligand has a significant impact on promoting a conformational change at the active site level. The effect, however, was different in the two chains (Fig. S6). In chain A, a significant lowering of H2 was observed, causing the opening of the backward access to the active site (supposed to be exploited by 4Ms compounds), while L2 (which regulates the entrance of E1) approached H1 slightly. In chain B, H2' moved in the opposite direction to chain A and induced the displacement of both L2' and H2', causing the active site to shrink. The closure of the gate that is thought to be the access route for E1 reinforced the hypothesis that compound 5 may behave as a non-competitive inhibitor that binds an alternative site at the dimer interface.

4. Discussion

Herein it is provided the first experimental proof of the existence of a sharp distinction between the dual zymosterone-reductase and steroid-hormone-ketoreductase activities of human enzyme HSD17B7.

The existence of multiple enzymatic activities in proteins that belong to the HSD17B superfamily is not unusual. In fact, several enzymes that are capable of reducing the keto group at the C-17 position of the steroid nucleus also display some reductase activity on the C-3 position [9]. Furthermore, many HSD17Bs display catalytical activities other than ketoreductase activity (e.g.: processing thioesters of carboxylic acids) on non-steroid substrates [42,43]. HSD17B7, however, possesses a unique feature: it plays the role as ketoreductase in the path that builds the molecule, cholesterol, from which all the steroid hormones are generated through a network of reaction that involves HSD17B7 itself and other ketoreductase enzymes. In

CHILD, Congenital hemidysplasia with ichthyosiform erythroderma and limb defects; DHT, dihydrotestosterone; E1, estrone; E2, estradiol; Erg27p, yeast 3-ketosteroid reductase; *ERG27,* gene encoding yeast 3-ketosteroid reductase; 17β-HSDs, 17β-hydroxysteroid dehydrogenases; HSD17B1, 17β-hydroxysteroid dehydrogenase type 1; HSD17B7, 17β-hydroxysteroid dehydrogenase type 7; 4-MZs, 4-methylzymosterone; 4-MFs, 4-methylfecosterone; Zs, zymosterone NSDHL, NADH sterol dehydrogenase-like; OS, 2,3-oxidosqualene; OSC, oxidosqualene cyclase; P, progesterone; SC4MOL, sterol C-4 methyl oxidase-like; SRD, short-chain dehydrogenase/reductase

short, the enzyme acts before and after the formation of cholesterol. In cholesterol biosynthesis, its ketoreductase activity restores the 3-β hydroxyl group temporarily lost during C-4 demethylation process. Indeed, C-4 demethylase sterol-biosynthesis apparatus is made up of three enzymes (C-4 methyl oxidase, C-4 decarboxylase and 3-ketosteroid reductase) and a protein (Ergosterol biosynthetic protein 28) that is thought to play a coordination role [44,45]. Interestingly, this *cluster condition* appears to be an ancestral condition as it is also found in other ancient organisms, such as plants, fungi and yeasts, in which the sterol-biosynthesis pathway is present. In yeasts, the four proteins appear to form a true enzymatic complex in which three enzymes are tethered by a scaffold protein [46]. It is noteworthy that sterol biosynthesis is a metabolic process that preceded, evolutionarily, the steroid-hormone metabolism.

To directly compare the catalytic activity of human HSD17B7 with different substrates in the absence of strongly disturbing background activities, *E. coli* was selected as the expression system. Recombinant human HSD17B7 was found to be highly active both as a zymosterone reductase and as a steroid-hormone reductase. As zymosterone reductase, we have here shown that it is able to convert not only the Zs in zymosterol but also the 4-MZs in the 4-methylzymosterol (as e.g. expected from the observation of Stottmann *et al* [11]).This enzyme's E1-reductase activity has elicited the attention of researchers that are interested in designing novel molecules for the treatment of estrogen-dependent breast cancer [15,19,47]. Indeed, HSD17B7 is overexpressed in breast cancer [15], and a series of powerful inhibitors have been investigated as possible anticancer agents [19]. Another source of interest for researchers was the fact that an absence of HSD17B7 in animal models causes embryo defects similar to those observed in some cholesterol disorders [12,48]. Stottmann *et al.* [11] have shown that an abnormal embryo phenotype was attributed to the toxicity of accumulated 4-MZs towards the Hedgehog proteins, which are critical for embryo development.

CHILD, Congenital hemidysplasia with ichthyosiform erythroderma and limb defects; DHT, dihydrotestosterone; E1, estrone; E2, estradiol; Erg27p, yeast 3-ketosteroid reductase; *ERG27,* gene encoding yeast 3-ketosteroid reductase; 17β-HSDs, 17β-hydroxysteroid dehydrogenases; HSD17B1, 17β-hydroxysteroid dehydrogenase type 1; HSD17B7, 17β-hydroxysteroid dehydrogenase type 7; 4-MZs, 4-methylzymosterone; 4-MFs, 4-methylfecosterone; Zs, zymosterone NSDHL, NADH sterol dehydrogenase-like; OS, 2,3-oxidosqualene; OSC, oxidosqualene cyclase; P, progesterone; SC4MOL, sterol C-4 methyl oxidase-like; SRD, short-chain dehydrogenase/reductase

As it was interesting in mimicking zymosterone-reductase deficiency by inhibiting the enzyme, it was deemed reasonable to assay the effects of known inhibitors of E1-reductase activity of HSD17B7 [19] on the zymosterone-reductase activity of the same enzyme.

A series of known HSD17B7 inhibitors (INH-1, 2 and 3) [19] was initially tested in cells (human hepatoma HepG2), which were incubated with radioactive acetate. Surprisingly, no accumulation of radioactive 4-MZs was detected in the non-saponifiable fraction that was extracted from treated cells, although higher concentrations than those that had proven to be effective as inhibitors of E1-reductase activity were used.

It appears that the potent specific inhibitors of the E1-reductase activity of HSD17B7 were ineffective as inhibitors of zymosterone-reductase activity. The molecules' ineffectiveness was confirmed by the incubation of hepatoma-cell lysates with radioactive 4-MZs in the presence of inhibitors; enzyme activity was found to be comparable to that of the control assay for all inhibitors (Table 2).

In order to further understand, on a molecular level, the difference in the inhibitory effects on the two enzymatic activities (zymosterone-reductase and hormone-ketosteroid-reductase activity) of human HSD17B7, the recombinant enzyme, overexpressed in *E. coli*, was tested towards the inhibitors, as reported in Fig. 3. Bacterial cells were chosen as the proper expression system as they lack any reductase activity towards E1. Furthermore, bacterial cells are not equipped with a sterol-biosynthesis enzyme pool, meaning that their cellular environment is presumed to be free from possible sterol-metabolism interference. As shown by the results reported in Table 5, the zymosterone-reductase activity of the enzyme proved to be essentially unaffected by the inhibitors, whereas all three hormone-reductase activities appeared to be inhibited (highly, in some cases) in the presence of the compounds which behave as mixed or non-competitive inhibitors. Comparable to another example from the literature [39], a possible alternative site at the dimer interface was identified to which the inhibitors may bind. The first MD analyses performed on the modelled free and liganded forms of the protein highlighted the fact that the ligand had a strong effect on overall protein stability and, in particular, on the active site of both monomers. This might suggest that the

CHILD, Congenital hemidysplasia with ichthyosiform erythroderma and limb defects; DHT, dihydrotestosterone; E1, estrone; E2, estradiol; Erg27p, yeast 3-ketosteroid reductase; *ERG27,* gene encoding yeast 3-ketosteroid reductase; 17β-HSDs, 17β-hydroxysteroid dehydrogenases; HSD17B1, 17β-hydroxysteroid dehydrogenase type 1; HSD17B7, 17β-hydroxysteroid dehydrogenase type 7; 4-MZs, 4-methylzymosterone; 4-MFs, 4-methylfecosterone; Zs, zymosterone NSDHL, NADH sterol dehydrogenase-like; OS, 2,3-oxidosqualene; OSC, oxidosqualene cyclase; P, progesterone; SC4MOL, sterol C-4 methyl oxidase-like; SRD, short-chain dehydrogenase/reductase

compounds may behave as a mixed or non-competitive inhibitors that are able to affect the accessibility of the protein active site by E1 and 4-MZs substrates in different ways. While E1 is known to enter the catalytic cavity through the frontal gate that is delimited by H1 and L2 [37], 4-MZs may exploit a backward access, which is regulated by the C-terminal helix. The different effects on these structural elements provided by the ligand might explain the different inhibitory effects on E1 and zymosterone-reductase activity that have been observed.

5. Conclusions

The inhibition experiments with molecules that are known E1-reductase inhibitors confirmed that human HSD17B7 presents two, functionally separate, enzymatic activities. Steroid-hormone-reductase activity (shared with mammals) is sensitive to inhibitors, while zymosterone-reductase activity (shared with all eukaryotes that possess a mevalonic pathway that forms sterols) is insensitive to inhibitors Molecular dynamic simulations suggest that an alternative binding site, located at the dimer interface, is able to host the tested inhibitors, which might then alter the dynamics of the structural elements that regulate access to the binding site by the different substrates, thus impeding E1 entrance while allowing access to 4-MZs.

The dual enzymatic activities of mammalian HSD17B7 make the protein a fully-fledged multifunctional protein and raise an intriguing question as to its evolutionary history; when, and thanks to which residues, did the zymosterone reductase which is present in all sterol-forming eukaryotes, learn its second job - E1 reductase activity? A careful comparison of all the known sequences of this protein should provide the first clues. Such a comparison will also shed light onto another question that is related to the evolution of the protein; indeed, yeast Erg27p, the orthologue of HSD17B7 belonging to the ergosterol biosynthesis as a 3-ketoreductase, behaves as a true moonlighting protein in that it protects OSC as its second function [49]. It would be interesting to establish whether the gain of hormone-reductase activity (the second function in

CHILD, Congenital hemidysplasia with ichthyosiform erythroderma and limb defects; DHT, dihydrotestosterone; E1, estrone; E2, estradiol; Erg27p, yeast 3-ketosteroid reductase; *ERG27,* gene encoding yeast 3-ketosteroid reductase; 17β-HSDs, 17β-hydroxysteroid dehydrogenases; HSD17B1, 17β-hydroxysteroid dehydrogenase type 1; HSD17B7, 17β-hydroxysteroid dehydrogenase type 7; 4-MZs, 4-methylzymosterone; 4-MFs, 4-methylfecosterone; Zs, zymosterone NSDHL, NADH sterol dehydrogenase-like; OS, 2,3-oxidosqualene; OSC, oxidosqualene cyclase; P, progesterone; SC4MOL, sterol C-4 methyl oxidase-like; SRD, short-chain dehydrogenase/reductase

mammals) occurred at the same time as the loss of OSC-protecting activity (the second job in yeasts) in ergosterol-forming eukaryotes (yeast and fungi).

Author contributions

T.F. and S.O.B. conceived and designed the experiments. T.F. performed the biological experiments and analysed the data. G.D. and F.S. performed the computational simulations and analysed the data. M.L.L. and D.P. contributed reagents/materials/analysis tools. M.D., S.A., G.B., F.S. and S.O.B wrote the manuscript, G.B. and S.O.B. supervised the project.

Competing financial interest

The authors declare no competing financial interest.

Acknowledgments

We thank Prof. J. Adamski (Institute of Experimental Genetics, Genome Analysis Centre, Neuherberg, Germany) for supplying the plasmid coding for human HSD17B7.

We kindly acknowledge the Centro di Competenza sul Calcolo Scientifico (C3S) at the University of Turin (c3s.unito.it) for providing the computational time and resources, and BiKi Technologies for providing the BiKi LiFe Sciences suite.

This work was financially supported by the University of Turin (Ricerca Locale ex 60% grants 2015-2018).

References

[1] S. Marchais-Oberwinkler, C. Henn, G. Möller, T. Klein, M. Negri, A. Oster, A. Spadaro, R. Werth, M. Wetzel, K. Xu, M. Frotscher, R.W. Hartmann, J. Adamski, 17β-Hydroxysteroid dehydrogenases (17β-HSDs) as

CHILD, Congenital hemidysplasia with ichthyosiform erythroderma and limb defects; DHT, dihydrotestosterone; E1, estrone; E2, estradiol; Erg27p, yeast 3-ketosteroid reductase; *ERG27,* gene encoding yeast 3-ketosteroid reductase; 17β-HSDs, 17β-hydroxysteroid dehydrogenases; HSD17B1, 17β-hydroxysteroid dehydrogenase type 1; HSD17B7, 17β-hydroxysteroid dehydrogenase type 7; 4-MZs, 4-methylzymosterone; 4-MFs, 4-methylfecosterone; Zs, zymosterone NSDHL, NADH sterol dehydrogenase-like; OS, 2,3-oxidosqualene; OSC, oxidosqualene cyclase; P, progesterone; SC4MOL, sterol C-4 methyl oxidase-like; SRD, short-chain dehydrogenase/reductase

therapeutic targets: Protein structures, functions, and recent progress in inhibitor development, Journal of Steroid Biochemistry and Molecular Biology 125 (2011) 66-82.
[2] P. Lukacik, K.L. Kavanagh, U. Oppermann, Structure and function of human 17β-hydroxysteroid dehydrogenases, Molecular and Cellular Endocrinology 248 (2006) 61-71.
[3] U. Oppermann, C. Filling, M. Hult, N. Shafqat, X.Q. Wu, M. Lindh, J. Shafqat, E. Nordling, Y. Kallberg, B. Persson, H. Jornvall, Short-chain dehydrogenases/reductases (SDR): the 2002 update, Chemico-Biological Interactions 143 (2003) 247-253.
[4] W. Rachel Duan, D.I.H. Linzer, G. Gibori, Cloning and characterization of an ovarian-specific protein that associates with the short form of the prolactin receptor, Journal of Biological Chemistry 271 (1996) 15602-15607.
[5] P. Nokelainen, H. Peltoketo, R. Vihko, P. Vihko, Expression cloning of a novel estrogenic mouse 17β-hydroxysteroid dehydrogenase/17-ketosteroid reductase (m17HSD7), previously described as a prolactin receptor-associated protein (PRAP) in rat, Molecular Endocrinology 12 (1998) 1048-1059.
[6] A. Krazeisen, R. Breitling, K. Imai, S. Fritz, G. Möller, J. Adamski, Determination of cDNA, gene structure and chromosomal localization of the novel human 17β-hydroxysteroid dehydrogenase type 7, FEBS Letters 460 (1999) 373-379.
[7] R. Breitling, A. Krazeisen, G. Möller, J. Adamski, 17β-hydroxysteroid dehydrogenase type 7 - An ancient 3-ketosteroid reductase of cholesterogenesis, Molecular and Cellular Endocrinology 171 (2001) 199-204.
[8] C.-Y. Zhang, W.-Q. Wang, J. Chen, S.-X. Lin, Reductive 17beta-hydroxysteroid dehydrogenases which synthesize estradiol and inactivate dihydrotestosterone constitute major and concerted players in ER+ breast cancer cells, The Journal of Steroid Biochemistry and Molecular Biology 150 (2015) 24-34.
[9] S. Törn, P. Nokelainen, R. Kurkela, A. Pulkka, M. Menjivar, S. Ghosh, M. Coca-Prados, H. Peltoketo, V. Isomaa, P. Vihko, Production, purification, and functional analysis of recombinant human and mouse 17β-hydroxysteroid dehydrogenase type 7, Biochemical and Biophysical Research Communications 305 (2003) 37-45.
[10] Z. Marijanovic, D. Laubner, G. Möller, C. Gege, B. Husen, J. Adamski, R. Breitling, Closing the gap: Identification of human 3-ketosteroid reductase, the last unknown enzyme of mammalian cholesterol biosynthesis, Molecular Endocrinology 17 (2003) 1715-1725.
[11] R.W. Stottmann, A. Turbe-Doan, P. Tran, L.E. Kratz, J.L. Moran, R.I. Kelley, D.R. Beier, Cholesterol metabolism is required for intracellular Hedgehog signal transduction in vivo, PLoS Genetics 7 (2011).
[12] F.D. Porter, G.E. Herman, Malformation syndromes caused by disorders of cholesterol synthesis, Journal of Lipid Research 52 (2011) 6-34.
[13] M. He, L.E. Kratz, J.J. Michel, A.N. Vallejo, L. Ferris, R.I. Kelley, J.J. Hoover, D. Jukic, K.M. Gibson, L.A. Wolfe, D. Ramachandran, M.E. Zwick, J. Vockley, Mutations in the human SC4MOL gene encoding a methyl sterol oxidase cause psoriasiform dermatitis, microcephaly, and developmental delay, Journal of Clinical Investigation 121 (2011) 976-984.
[14] G.E. Herman, Disorders of cholesterol biosynthesis: Prototypic metabolic malformation syndromes, Human Molecular Genetics 12 (2003) R75-R88.
[15] A. Shehu, J. Mao, G.B. Gibori, J. Halperin, J. Le, Y.S. Devi, B. Merrill, H. Kiyokawa, G. Gibori, Prolactin receptor-associated protein/17β-hydroxysteroid dehydrogenase type 7 gene (Hsd17b7) plays a crucial role in embryonic development and fetal survival, Molecular Endocrinology 22 (2008) 2268-2277.
[16] H. Jokela, P. Rantakari, T. Lamminen, L. Strauss, R. Ola, A.L. Mutka, H. Gylling, T. Miettinen, P. Pakarinen, K. Sainio, M. Poutanen, Hydroxysteroid (17β) dehydrogenase 7 activity is essential for fetal de novo cholesterol synthesis and for neuroectodermal survival and cardiovascular differentiation in early mouse embryos, Endocrinology 151 (2010) 1884-1892.

CHILD, Congenital hemidysplasia with ichthyosiform erythroderma and limb defects; DHT, dihydrotestosterone; E1, estrone; E2, estradiol; Erg27p, yeast 3-ketosteroid reductase; *ERG27,* gene encoding yeast 3-ketosteroid reductase; 17β-HSDs, 17β-hydroxysteroid dehydrogenases; HSD17B1, 17β-hydroxysteroid dehydrogenase type 1; HSD17B7, 17β-hydroxysteroid dehydrogenase type 7; 4-MZs, 4-methylzymosterone; 4-MFs, 4-methylfecosterone; Zs, zymosterone NSDHL, NADH sterol dehydrogenase-like; OS, 2,3-oxidosqualene; OSC, oxidosqualene cyclase; P, progesterone; SC4MOL, sterol C-4 methyl oxidase-like; SRD, short-chain dehydrogenase/reductase

[17] S. Fillinger, P. Leroux, C. Auclair, C. Barreau, C. Al Hajj, D. Debieu, Genetic analysis of fenhexamid-resistant field isolates of the phytopathogenic fungus Botrytis cinerea, Antimicrobial Agents and Chemotherapy 52 (2008) 3933-3940.
[18] C. Albertini, P. Leroux, A Botrytis cinerea putative 3-keto reductase gene (ERG27) that is homologous to the mammalian 17β-hydroxysteroid dehydrogenase type 7 gene (17β-HSD7), European Journal of Plant Pathology 110 (2004) 723-733.
[19] E. Bellavance, V. Luu-The, D. Poirier, Potent and selective steroidal inhibitors of 17β-hydroxysteroid dehydrogenase type 7, an enzyme that catalyzes the reduction of the key hormones estrone and dihydrotestosterone, Journal of Medicinal Chemistry 52 (2009) 7488-7502.
[20] D. Poirier, Contribution to the development of inhibitors of 17β-hydroxysteroid dehydrogenase types 1 and 7: Key tools for studying and treating estrogen-dependent diseases, Journal of Steroid Biochemistry and Molecular Biology 125 (2011) 83-94.
[21] T. Ferrante, A. Barge, S. Taramino, S. Oliaro-Bosso, G. Balliano, 4-Methylzymosterone and Other Intermediates of Sterol Biosynthesis from Yeast Mutants Engineered in the ERG27 Gene Encoding 3-Ketosteroid Reductase, Lipids 51 (2016) 1103-1113.
[22] M. Keller, A. Wolfgardt, C. Müller, R. Wilcken, F.M. Böckler, S. Oliaro-Bosso, T. Ferrante, G. Balliano, F. Bracher, Arylpiperidines as a new class of oxidosqualene cyclase inhibitors, European Journal of Medicinal Chemistry 109 (2016) 13-22.
[23] S. Oliaro-Bosso, S. Taramino, F. Viola, S. Tagliapietra, G. Ermondi, G. Cravotto, G. Balliano, Umbelliferone aminoalkyl derivatives as inhibitors of human oxidosqualene-lanosterol cyclase, Journal of Enzyme Inhibition and Medicinal Chemistry 24 (2009) 589-598.
[24] B.E. Cham, B.R. Knowles, A solvent system for delipidation of plasma or serum without protein precipitation, Journal of Lipid Research 17 (1976) 176-181.
[25] D. Schuster, D. Kowalik, J. Kirchmair, C. Laggner, P. Markt, C. Aebischer-Gumy, F. Ströhle, G. Möller, G. Wolber, T. Wilckens, T. Langer, A. Odermatt, J. Adamski, Identification of chemically diverse, novel inhibitors of 17β-hydroxysteroid dehydrogenase type 3 and 5 by pharmacophore-based virtual screening, Journal of Steroid Biochemistry and Molecular Biology 125 (2011) 148-161.
[26] A. Waterhouse, M. Bertoni, S. Bienert, G. Studer, G. Tauriello, R. Gumienny, F.T. Heer, T.A.P. De Beer, C. Rempfer, L. Bordoli, R. Lepore, T. Schwede, SWISS-MODEL: Homology modelling of protein structures and complexes, Nucleic Acids Research 46 (2018) W296-W303.
[27] M.W. Sawicki, M. Erman, T. Puranen, P. Vihko, D. Ghosh, Structure of the ternary complex of human 17β-hydroxysteroid dehydrogenase type 1 with 3-hydroxyestra-1,3,5,7-tetraen-17-one (equilin) and NADP+, Proceedings of the National Academy of Sciences 96 (1999) 840-845.
[28] G. Jones, P. Willett, R.C. Glen, A.R. Leach, R. Taylor, Development and validation of a genetic algorithm for flexible docking, Journal of Molecular Biology 267 (1997) 727-748.
[29] E.L. D. van der Spoel, B. Hess, and the GROMACS development team, GROMACS User Manual version 4.6.5, www.gromacs.org, 2013.
[30] V. Hornak, R. Abel, A. Okur, B. Strockbine, A. Roitberg, C. Simmerling, Comparison of multiple amber force fields and development of improved protein backbone parameters, Proteins: Structure, Function and Genetics 65 (2006) 712-725.
[31] W.L. Jorgensen, J. Chandrasekhar, J.D. Madura, R.W. Impey, M.L. Klein, Comparison of simple potential functions for simulating liquid water, The Journal of Chemical Physics 79 (1983) 926-935.
[32] H.J. Berendsen, S. Hayward, Collective protein dynamics in relation to function, Current Opinion in Structural Biology 10 (2000) 165-169.
[33] F. Maione, S. Oliaro-Bosso, C. Meda, F. Di Nicolantonio, F. Bussolino, G. Balliano, F. Viola, E. Giraudo, The cholesterol biosynthesis enzyme oxidosqualene cyclase is a new target to impair tumour angiogenesis and metastasis dissemination, Scientific Reports 5 (2015).

CHILD, Congenital hemidysplasia with ichthyosiform erythroderma and limb defects; DHT, dihydrotestosterone; E1, estrone; E2, estradiol; Erg27p, yeast 3-ketosteroid reductase; *ERG27,* gene encoding yeast 3-ketosteroid reductase; 17β-HSDs, 17β-hydroxysteroid dehydrogenases; HSD17B1, 17β-hydroxysteroid dehydrogenase type 1; HSD17B7, 17β-hydroxysteroid dehydrogenase type 7; 4-MZs, 4-methylzymosterone; 4-MFs, 4-methylfecosterone; Zs, zymosterone NSDHL, NADH sterol dehydrogenase-like; OS, 2,3-oxidosqualene; OSC, oxidosqualene cyclase; P, progesterone; SC4MOL, sterol C-4 methyl oxidase-like; SRD, short-chain dehydrogenase/reductase

[34] Y. Liang, C. Besch-Williford, J.D. Aebi, B. Mafuvadze, M.T. Cook, X. Zou, S.M. Hyder, Cholesterol biosynthesis inhibitors as potent novel anti-cancer agents: Suppression of hormone-dependent breast cancer by the oxidosqualene cyclase inhibitor RO 48-8071, Breast Cancer Research and Treatment 146 (2014) 51-62.
[35] D. Gachotte, S.E. Sen, J. Eckstein, R. Barbuch, M. Krieger, B.D. Ray, M. Bard, Characterization of the Saccharomyces cerevisiae ERG27 gene encoding the 3-keto reductase involved in C-4 sterol demethylation, Proceedings of the National Academy of Sciences 96 (1999) 12655-12660.
[36] J.T.Moore, J.L. Gaylor, Investigation of an S-Adenosylmethionine:Δ24-Sterol Methyltransferase in Ergosterol Biosynthesis in Yeast, J Biol Chem (1970) 4684-4688.
[37] M. Negri, M. Recanatini, R.W. Hartmann, Insights in 17β-HSD1 enzyme kinetics and ligand binding by dynamic motion investigation, PLoS ONE 5 (2010).
[38] M. Baroni, G. Cruciani, S. Sciabola, F. Perruccio, J.S. Mason, A common reference framework for analyzing/comparing proteins and ligands. Fingerprints for ligands and proteins (FLAP): Theory and application, Journal of Chemical Information and Modeling 47 (2007) 279-294.
[39] P.J.A. Michiels, C. Ludwig, M. Stephan, C. Fischer, G. Möller, J. Messinger, M. van Dongen, H. Thole, J. Adamski, U.L. Günther, Ligand-based NMR spectra demonstrate an additional phytoestrogen binding site for 17β-hydroxysteroid dehydrogenase type 1, The Journal of Steroid Biochemistry and Molecular Biology 117 (2009) 93-98.
[40] L. Siragusa, S. Cross, M. Baroni, L. Goracci, G. Cruciani, BioGPS: Navigating biological space to predict polypharmacology, off-targeting, and selectivity, Proteins: Structure, Function and Bioinformatics 83 (2015) 517-532.
[41] A. Amadei, A.B.M. Linssen, H.J.C. Berendsen, Essential dynamics of proteins, Proteins: Structure, Function, and Bioinformatics 17 (1993) 412-425.
[42] J.K. Hiltunen, A.J. Kastaniotis, K.J. Autio, G. Jiang, Z. Chen, T. Glumoff, 17B-hydroxysteroid dehydrogenases as acyl thioester metabolizing enzymes, Molecular and Cellular Endocrinology 489 (2019) 107-118.
[43] P. Rantakari, H. Lagerbohm, M. Kaimainen, J.P. Suomela, L. Strauss, K. Sainio, P. Pakarinen, M. Poutanen, Hydroxysteroid (17β) dehydrogenase 12 is essential for mouse organogenesis and embryonic survival, Endocrinology 151 (2010) 1893-1901.
[44] C. Ottolenghi, I. Daizadeh, A. Ju, S. Kossida, G. Renault, M. Jacquet, A. Fellous, W. Gilbert, R. Veitia, The genomic structure of C14orf1 is conserved across eukarya, Mammalian Genome 11 (2000) 786-788.
[45] D. Gachotte, J. Eckstein, R. Barbuch, T. Hughes, C. Roberts, M. Bard, A novel gene conserved from yeast to humans is involved in sterol biosynthesis, Journal of Lipid Research 42 (2001) 150-154.
[46] C. Mo, M. Bard, Erg28p is a key protein in the yeast sterol biosynthetic enzyme complex, Journal of Lipid Research 46 (2005) 1991-1998.
[47] A. Shehu, C. Albarracin, Y. Sangeeta Devi, K. Luther, J. Halperin, J. Le, J. Mao, R.W. Duan, J. Frasor, G. Gibori, The stimulation of hsd17b7 expression by estradiol provides a powerful feed-forward mechanism for estradiol biosynthesis in breast cancer cells, Molecular Endocrinology 25 (2011) 754-766.
[48] T. Saloniemi, H. Jokela, L. Strauss, P. Pakarinen, M. Poutanen, The diversity of sex steroid action: Novel functions of hydroxysteroid (17β) dehydrogenases as revealed by genetically modified mouse models, Journal of Endocrinology 212 (2012) 27-40.
[49] C. Mo, P. Milla, K. Athenstaedt, R. Ott, G. Balliano, G. Daum, M. Bard, In yeast sterol biosynthesis the 3-keto reductase protein (Erg27p) is required for oxidosqualene cyclase (Erg7p) activity, Biochimica et Biophysica Acta - Molecular and Cell Biology of Lipids 1633 (2003) 68-74.

CHILD, Congenital hemidysplasia with ichthyosiform erythroderma and limb defects; DHT, dihydrotestosterone; E1, estrone; E2, estradiol; Erg27p, yeast 3-ketosteroid reductase; *ERG27,* gene encoding yeast 3-ketosteroid reductase; 17β-HSDs, 17β-hydroxysteroid dehydrogenases; HSD17B1, 17β-hydroxysteroid dehydrogenase type 1; HSD17B7, 17β-hydroxysteroid dehydrogenase type 7; 4-MZs, 4-methylzymosterone; 4-MFs, 4-methylfecosterone; Zs, zymosterone NSDHL, NADH sterol dehydrogenase-like; OS, 2,3-oxidosqualene; OSC, oxidosqualene cyclase; P, progesterone; SC4MOL, sterol C-4 methyl oxidase-like; SRD, short-chain dehydrogenase/reductase